95

CENT
DO

MARTIN MARIETTA ENERGY SYSTEMS LIBRARIES
3 4456 0364461 6

ORNL-3209
UC-80 – Reactor Technology
TID-4500 (41st ed.)

A COMPARISON OF GAS-TURBINE AND STEAM-TURBINE POWER PLANTS FOR USE WITH ALL-CERAMIC GAS-COOLED REACTORS

A. P. Fraas
M. N. Ozisik

OAK RIDGE NATIONAL LABORATORY
operated by
UNION CARBIDE CORPORATION
for the
U.S. ATOMIC ENERGY COMMISSION

CENTRAL RESEARCH LIBRARY
DOCUMENT COLLECTION
LIBRARY LOAN COPY
DO NOT TRANSFER TO ANOTHER PERSON
If you wish someone else to see this document, send in name with document and the library will arrange a loan.

Printed in USA. Price $3.00. Available from the Clearinghouse for Federal Scientific and Technical Information, National Bureau of Standards, U.S. Department of Commerce, Springfield, Virginia

LEGAL NOTICE

This report was prepared as an account of Government sponsored work. Neither the United States, nor the Commission, nor any person acting on behalf of the Commission:

A. Makes any warranty or representation, expressed or implied, with respect to the accuracy, completeness, or usefulness of the information contained in this report, or that the use of any information, apparatus, method, or process disclosed in this report may not infringe privately owned rights; or

B. Assumes any liabilities with respect to the use of, or for damages resulting from the use of any information, apparatus, method, or process disclosed in this report.

As used in the above, "person acting on behalf of the Commission" includes any employee or contractor of the Commission, or employee of such contractor, to the extent that such employee or contractor of the Commission, or employee of such contractor prepares, disseminates, or provides access to, any information pursuant to his employment or contract with the Commission, or his employment with such contractor.

ORNL-3209

Contract No. W-7405-eng-26

Reactor Division

A COMPARISON OF GAS-TURBINE AND STEAM-TURBINE POWER PLANTS FOR USE WITH ALL-CERAMIC GAS-COOLED REACTORS

A. P. Fraas M. N. Ozisik

JULY 1965

OAK RIDGE NATIONAL LABORATORY
Oak Ridge, Tennessee
operated by
UNION CARBIDE CORPORATION
for the
U.S. ATOMIC ENERGY COMMISSION

MARTIN MARIETTA ENERGY SYSTEMS LIBRARIES

3 4456 0364461 6

CONTENTS

	Page
Abstract	1
Introduction	2
Conclusions	3
Selection of Design Conditions	5
Turbine Inlet Temperature	8
Compressor Inlet Temperature	9
Regeneration and Intercooling	9
Evaluation Procedure	12
Effects of Major Parameters on the Cycle Efficiency	12
Effects of Regenerator Design on Cycle Performance and Costs	16
Effects of Heat Exchanger Proportions on Costs	17
Effects of Turbine-Compressor Units on Costs	23
Effects of Reactor Design Parameters on Fuel-Cycle Costs	24
Effects of Pressure Losses and Regenerator Effectiveness on Costs	29
Effects of Turbine Inlet Temperature on Costs	40
Computer Codes	41
Plant Layout	45
General Requirements	45
Configuration Studies	47
Reference Design (HGCR-6)	48
Comparison of Steam- and Gas-Turbine Plants	50
Costs	51
Maintenance	51
Hazards	54
Thermal Efficiency	54
Application of More Complex Gas-Turbine Systems	55
References	56
Nomenclature	58

Appendix A. Cycle Efficiency 63

Appendix B. Pumping Power-to-Heat Removal Ratio and Tube Length for a Counterflow Regenerator 65

Appendix C. Pumping Power-to-Heat Removal and Tube Length for a Counterflow Cooler with Constant Wall Temperature 72

Appendix D. Evaluation of the Heat Transfer Area for the Heat Exchangers 76

A COMPARISON OF GAS-TURBINE AND STEAM-TURBINE POWER PLANTS FOR USE WITH ALL-CERAMIC GAS-COOLED REACTORS

A. P. Fraas M. N. Ozisik

Abstract

The reactor outlet gas temperatures obtainable with metal encapsulated fuel have been too low to give an attractive gas-turbine installation, but with ceramic fuel elements the reactor outlet gas temperature could be as high as the permissible inlet temperature to any foreseeable gas turbine. This study compares gas turbines with steam turbines as a means of producing electric power from gas-cooled reactors with all-ceramic fuel elements.

The first portion of the study was a parametric investigation of gas-turbine power plants to investigate the effects of regeneration, pressure losses in components, system pressure level, and system operating temperatures. Earlier work on gas-cooled reactors was then utilized to select a good set of reactor core proportions, with due allowances for heat transfer and stress limitations, fuel-cycle costs, and reactor, pressure vessel, and shielding costs. Based on these proportions and data from the parametric survey, a series of eight power plant configurations was investigated and compared from the standpoint of costs, hazards problems, and maintenance. The best of these configurations was then chosen, and a conceptual design of a gas-turbine plant was prepared. The features, problems, and costs of this plant were then compared with those of a comparable steam-turbine plant.

The study indicates that a steam-turbine plant gives a higher thermal efficiency, lower initial capital charges, and substantially less-difficult maintenance problems than the gas-turbine plant. The heat exchanger equipment and duct work are much larger and the gas system is more complex in the gas-turbine plant. The lower thermal efficiency increases both the reactor size and the fuel-cycle costs. Perhaps the most important factor is that the turbine and compressor rotors in a gas-turbine plant are very large, heavy, and cumbersome. Since they would also pick up about 100 times as much activity as the rotors in the gas-circulating blowers for a steam plant, they would pose vastly more difficult maintenance problems.

Introduction

There has been much interest in coupling a gas turbine to a gas-cooled reactor because it appears that this might give a simpler power plant than can be achieved with a steam turbine and its related equipment. For mobile applications, such a plant has the further advantages that it appears to be lighter and, if the power regulation is achieved by varying the system pressure, its part-load efficiency is higher than that of a steam plant. For arctic or desert applications, it also has the advantage that it does not require any water in the system. Elimination of the water and hence possible steam leakage into the gas system eliminates both the consequent corrosion problems and the hazards associated with hydrogen formation from the water-gas reaction with graphite.

If the gas turbine is to be attractive for central station applications, the capital and fuel-cycle costs must be competitive with those of steam-turbine systems. This implies turbine inlet gas temperatures substantially higher than seem feasible for stainless steel-encapsulated UO_2 fuel elements. Recent studies[1] on the application of all-ceramic fuel elements to gas-cooled reactors of advanced types indicate that some of these show promise of giving marked reductions in the costs of producing power from the gas-cooled reactors, in part because of the higher permissible fuel operating temperatures. While the reactor designs of the studies were investigated primarily for steam-turbine power plants, they also appeared to be well suited to gas-turbine plants. This study was undertaken to investigate the application of the more promising of these reactors to gas-turbine plants and to evaluate the relative costs of power produced by steam and gas turbines from these gas-cooled reactors using as nearly comparable conditions as possible.

One of the most promising of the conceptual designs presented in ref. 1 for a gas-cooled reactor coupled to a steam-turbine power plant — the BeO-moderated, BeO-UO_2 fueled, HGCR-4 design — was used as the point of departure for the preparation of a conceptual design for a gas-turbine plant. To facilitate the work and provide as direct a comparison as possible, the same basic reactor configuration, fuel-handling system, and containment shell were employed in the gas-turbine plant designs covered

in this study. Since most of the reactor and nuclear plant problems are the same for the steam- and gas-turbine plants, to avoid repetition it was assumed that a reader of this report would have at hand and be familiar with ref. 1.

Conclusions

The first portion of the study was directed toward the preparation of tables and charts to show the effects on cycle efficiency of such parameters as turbine and compressor inlet temperatures, regenerator and cooler effectiveness, and pumping power losses in the reactor, heat exchangers, and ducting. The next portion of the study was concerned with the design of suitable heat exchangers. Heat transfer and stress limitations were established, and charts were developed for the cost and effectiveness of regenerators and coolers as functions of the principal design parameters. Plant layouts were prepared for six different arrangements of the major components in an effort to minimize the size and cost of the gas ducts and at the same time satisfy such other requirements as accommodation of differential thermal expansion, afterheat removal, etc. These charts, tables, and layouts were then used to estimate the effects of gas-turbine-cycle parameters on the cost of major components of the plant.

The most promising of the gas-turbine plants was selected and compared with a comparable steam-turbine plant. (The principal design parameters of these two plants are summarized in Table 1.) The study indicates that the heat exchangers, shielding, containment shell, and gas duct work for the most promising of the gas-turbine plants would be larger and would cost substantially more than the corresponding components for a steam-turbine plant. Further, the net thermal efficiency for the gas-turbine plant would be about 75% of that for the steam-turbine plant. Since the reactors would be basically similar, the lower cycle efficiency would make both the capital charges and the fuel-cycle costs about 25% higher for the gas-turbine plants.

Maintenance problems posed by a contaminated-gas system would probably not be serious in the heat exchanger equipment, since the probability

Table 1. Comparison of Design Data for Gas- and Steam-Turbine Power Plants Based on the HGCR-4 CO_2-Cooled Reactor

	Steam-Turbine Plant	Gas-Turbine Plant
Reactor thermal output, Mw	1170	1630
Net electrical output, Mw	500	500
Net overall efficiency, %	42.7	30.7
Reactor gas inlet temperature, °F	665	900
Reactor gas outlet temperature, °F	1250	1350
Reactor gas system pressure, psia	640	1000
Turbine inlet temperature, °F	1050	1350
Turbine inlet pressure, psia	2500	950
Turbine outlet temperature, °F	91.7	97.5
Turbine outlet pressure, psia	0.7	180

that such components would require replacement could be made exceedingly low. This does not seem to be the case for the gas circulators, however. Here the maintenance problem appears to be far more serious for the gas turbine and compressor than for the steam-turbine-driven gas-circulating blower of the corresponding steam-turbine plant. The gas-turbine cycle requires a compressor having many stages. Regeneration reduces the gas temperature rise through the reactor and increases the gas flow rate so that the compressor and turbine are larger in diameter and over ten times as long as the circulating blowers required for a system using a steam cycle. Not only is the surface area exposed to the contaminated gas greater, but the initial temperature drop in the gas system occurs in the turbine rather than a heat exchanger, and hence the amount of fission-product activity deposited in the turbine appears likely to be roughly 100 times greater than in a circulating blower. If the casing for the gas turbine were not split on the horizontal centerline, the bearing and stator support and assembly problems would require a complex double

casing, whereas for the steam plant the blower rotor assembly could be removed through a single circular flange separated from the hot portion of a simple casing by a heat dam. Thus the size and complexity of the moving parts exposed to the contaminated gas would lead to far more difficult design and maintenance problems in the gas turbine.

The gas-turbine plant also appears to be less attractive from the hazards standpoint. The much greater complexity of the duct system for the gas turbine presents more severe thermal expansion problems, which inherently reduce the integrity of the gas-system pressure envelope relative to that for the steam plant. The greater size and complexity of the turbine-compressor units makes them less reliable than the centrifugal blowers of a steam plant, and the greater complexity of the duct work makes thermal convection less effective in removing afterheat. On the other hand, if graphite is used as a moderator, reactions between steam and graphite, particularly those giving potentially hazardous amounts of hydrogen, are completely avoided in the gas-turbine plant.

Installing the turbine-generator units in the containment shell increases the size and cost of this component, but the added cost of the containment shell is roughly offset by elimination of the turbine building. However, hazards considerations would restrict maintenance operations within the containment shell, so the gas-turbine plant would be less attractive and probably more expensive.

Selection of Design Conditions

This study was conducted by taking the 500-Mw(e) HTGR-4 plant of ref. 1 as the reference design for a well-proportioned steam-turbine plant and comparing it with a series of gas-turbine plants for which the design conditions were varied in an effort to obtain a well-proportioned gas-turbine plant. The basic layout of the similar HGCR-5 plant is shown in Figs. 1 and 2. It should be mentioned that it was difficult to decide which of the two reactors should be used as the reference design — the HGCR-4, a CO_2-cooled, BeO-moderated reactor, or the HGCR-5, a helium-cooled, graphite-moderated reactor. The two designs are virtually the same. A few dimensional differences arose from small differences in

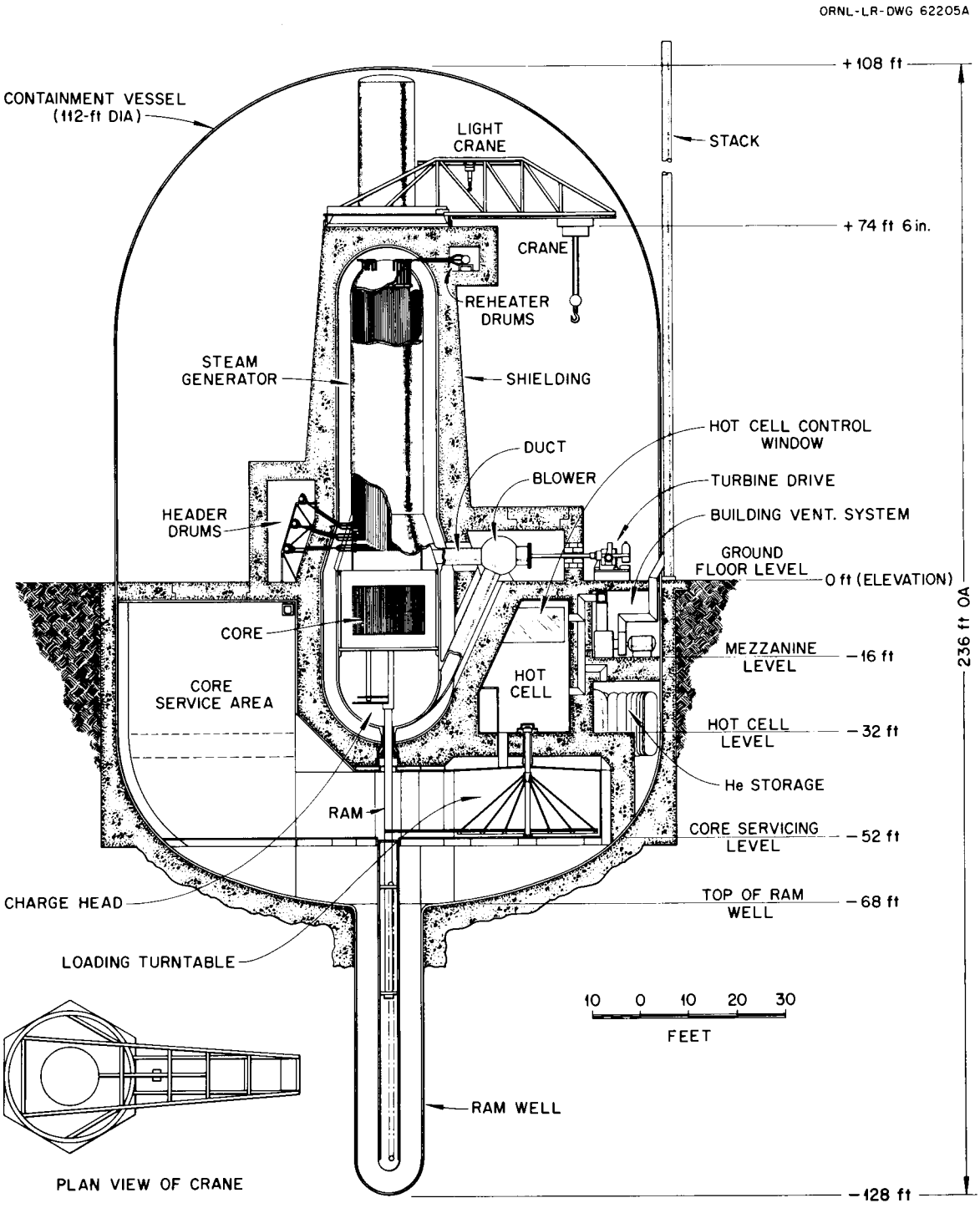

Fig. 1. Vertical Section Through HGCR-5.

ORNL-LR-DWG 63781

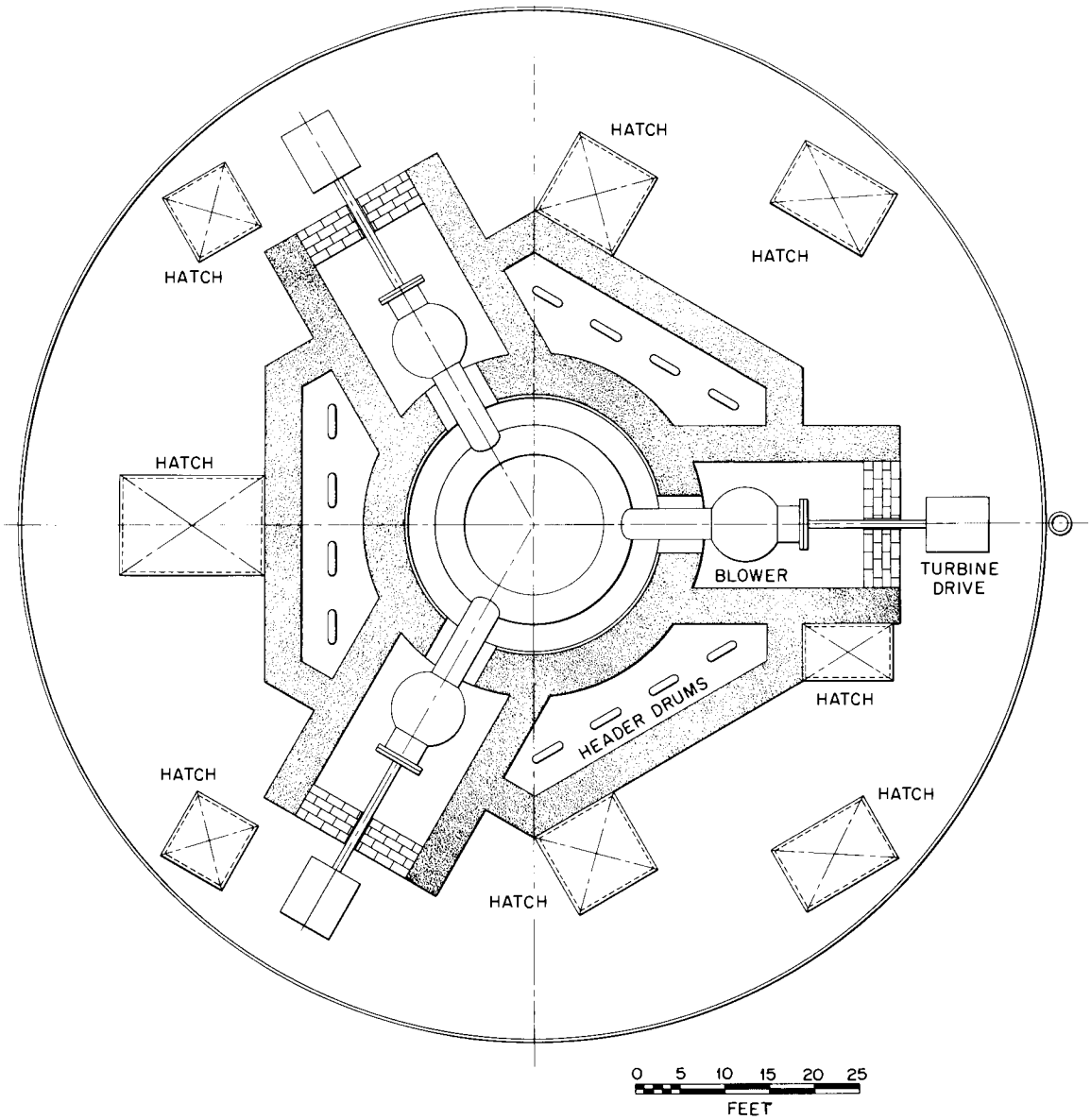

Fig. 2. Horizontal Section Through HGCR-5 at Ground Floor.

the heat transfer characteristics of helium and CO_2 and the lower atomic density of graphite as compared with BeO. The latter effect was the larger, and it gave a 3-ft-diam larger core and a 5-ft-diam larger reflector and pressure vessel for the graphite reactor. The BeO-CO_2 system of the HGCR-4 was chosen because it gave smaller and less expensive turbine-compressor units and hence gave a more promising gas-turbine plant.[2]

Fortunately, the major operating conditions for minimum costs appear to be much the same for the gas-turbine and steam-turbine plants. For example, in both cases the peak gas temperature is about as high as can be employed with the materials available, and the gas system pressure is limited by pressure vessel cost considerations. Similarly, the reactor core design was largely determined by fuel-cycle and reactor core capital cost considerations. Thus the range of reactor designs considered for the steam-turbine plant could be used with little modification for the gas-turbine study, and hence the reactor and fuel-cycle costs were directly comparable.

Turbine Inlet Temperature

The peak gas temperature chosen initially in the steam power plant study was 1350°F, although later work favored a temperature of 1200 to 1250°F. A higher value was not used because of the limitations imposed by the creep strength of steels suitable for the boiler tubes. While more refractory (and more expensive) alloys could be employed in the gas-turbine cycle, the nature of the system is such that the stresses in many components in the highest temperature region are higher than for the comparable steam-turbine system. This is especially true for the turbine buckets. Some gas-turbine manufacturers believe that a 1350°F turbine inlet temperature would be about as high as should be considered if a 20-yr life is to be required of units to be constructed in the 1965–1970 period. In view of this, and since the effects of increasing the turbine inlet temperature from 1350 to 1650°F were investigated and found to be small (the cycle efficiency increased only 3%), the gas temperature leaving the reactor was taken as 1350°F for the reference design.

From the long-range standpoint, gas turbine inlet temperatures higher than 1350°F could be employed by resorting to one or more devices. Molybdenum or niobium blades might be employed, but their oxidation resistance would still pose a problem at temperatures around 1500°F, even in helium with only a few parts per million of oxygen.[2] Just a few hundred parts per million of oxygen or water vapor would be likely to give serious trouble with niobium at temperatures above 800°F. There are indications

that molybdenum might be satisfactory in a reducing atmosphere (e.g., hydrogen or a helium-hydrogen mixture), but much experimental work will be required to demonstrate this.

Turbine-bucket cooling would permit an increase in the turbine inlet temperature, but experience in the turbojet engine field indicates that the pumping and eddy losses associated with flow from the bucket tips would offset much of the ideal gain in performance that might be expected.

Compressor Inlet Temperature

The performance of a gas turbine is very sensitive to the compressor inlet gas temperature. In the steam-turbine system it was assumed that condenser cooling water would be available at 70°F, and this appeared to be a good base condition for the gas-turbine plant. Perturbations were then applied to investigate the benefits that might accrue from operation of a gas-turbine plant in arctic regions and the losses in performance to be expected if it were to be operated in hot desert regions by considering compressor inlet temperatures ranging from 50 to 150°F. The temperature drops between the cycle gas and both cooling water and cooling air streams were found to be about 30 and 50°F, respectively, for well-proportioned heat exchangers.

Regeneration and Intercooling

A closed cycle with regeneration and one stage of intercooling in the compressor, as shown in Figs. 3 and 4, was chosen for analysis. It was essential to use a closed cycle because fission products leak from all-ceramic fuel elements and contaminate the gas stream. Even with metal-clad fuel elements, hazards considerations preclude an open cycle. While a closed cycle has the disadvantage that it entails the added cost of a cooler, it appears that the additional cost is much more than compensated by the reductions in the size and cost of the regenerator and reactor obtainable by going to a high-pressure gas system as opposed to a simple open cycle. (The minimum reactor capital cost for the steam-turbine plant appeared to be given by a gas system pressure of 500 to 1000 psi.) While more than one stage of intercooling is advantageous

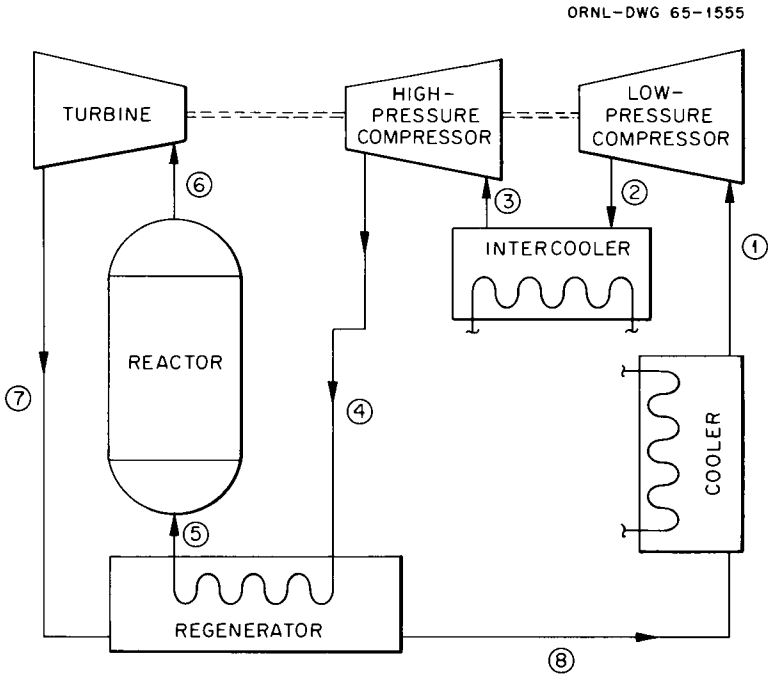

Fig. 3. Flow Diagram for the Direct-Cycle Gas-Turbine and Reactor.

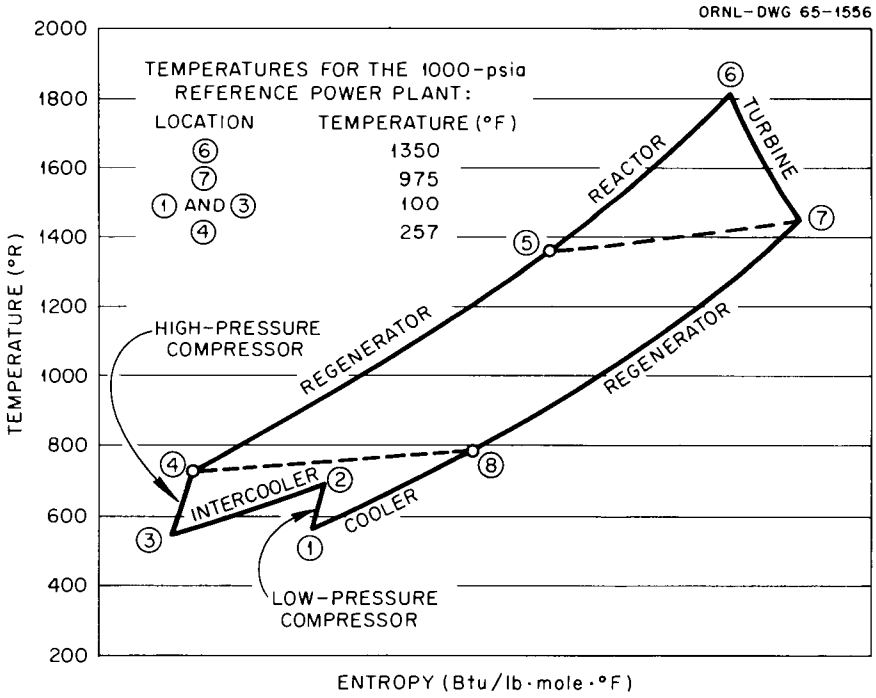

Fig. 4. Entropy Diagram for the Gas-Turbine Cycle.

in an idealized gas-turbine cycle, experience indicates that compressor entrance and exit losses and other factors offset much of this advantage in an actual unit. Hence the simpler single-stage intercooler was chosen for this study.

There are a host of other parameters which to some degree affect the performance, size, and cost of the system components. Wherever there was good reason to believe that the optimum value for one of these parameters fell in a broad region in which the overall system cost and performance are relatively insensitive to its variation, the parameter was fixed at a value in the region likely to be optimum. Earlier studies carried out by Packard,[3] General Atomic,[4] and Aerojet[5] were examined to justify the choice of the values chosen for the first phase of the work. This review indicated that one of the most important parameters that should be allowed to vary was the pumping power-to-heat removal ratio for both the regenerator and the cycle, since this factor had opposite effects on cycle performance and capital costs. Further cycle analysis work was carried out by hand calculations, and then a computing-machine code was worked out and used for additional studies. The latter work was carried out as a thesis study and is reported separately.[6] All these studies were consistent, and they indicated that there is little difference in cycle efficiency between helium and CO_2 and that the optimum compression ratio for a CO_2 cycle in this temperature range is about 5.5 to 1.

A peak system pressure of 1000 psia was chosen because it seemed to give close to minimum costs, although the overall power generation cost appears to be relatively insensitive to system pressure over the range from 500 to 1000 psi. While it was a bit inconsistent with the 685 psia chosen for the steam system and yielded a pressure vessel wall thickness in excess of 4 in., the lower costs associated with the higher pressure favored the gas-turbine system, and hence the change appeared to be in order. Temperatures of 1350°F at the turbine inlet (reactor outlet), 975°F at the turbine outlet, 100°F at the compressor inlet, and 257°F at the high-pressure compressor outlet were selected for the reference design. The associated compressor pressure ratio gave near-optimum cycle efficiencies for pumping power-to-heat removal ratios up to 9% and a

regenerator effectiveness between 70 and 90%. Perturbations were then applied to individual variables wherever the extra calculations appeared warranted. These perturbations included variations in the turbine inlet temperature from 1200 to 1650°F and the use of helium instead of CO_2.

Evaluation Procedure

The first steps in the study were the determination of the cycle efficiency for a variety of operating conditions, the preparation of basic generalized designs for the major components to facilitate the estimation of the effects of design conditions on their size and cost, and the establishment of specifications for the plant layout. A number of plant layouts were then prepared to investigate their relative advantages and disadvantages. Estimates of the effects of major design parameters on the costs of the heat exchangers, ducts, shield, and containment vessel were then made using the most promising configuration evolved. In all cases only the basic materials and fabrication costs were considered — no allowances were made for design, development, tooling, overhead, installation, or contingency. Therefore, the costs should be considered as relative rather than absolute costs. Experience with pressurized-water reactor plants indicates that the actual costs for a second- or third-generation plant would probably run about twice these basic costs for materials and fabrication labor.

Effects of Major Parameters on the Cycle Efficiency

Figures 5 and 6 show the basic cycle efficiency as a function of pumping power-to-heat removal ratio and the regenerator effectiveness for a 1000-psia CO_2 cycle with a 1350°F turbine inlet temperature and a 100°F compressor inlet temperature. Figure 7 shows the effects on the cycle efficiency of reactor outlet temperature (i.e., turbine inlet temperature) for the range from 1200 to 1650°F. The effect of compressor inlet temperature on the cycle efficiency is shown in Fig. 8. A compressor efficiency of 85% and a turbine efficiency of 90% were assumed for these calculations. The optimum compression ratio was about 5:1 for the 1200°F turbine inlet temperature, 90% regenerator effectiveness, and

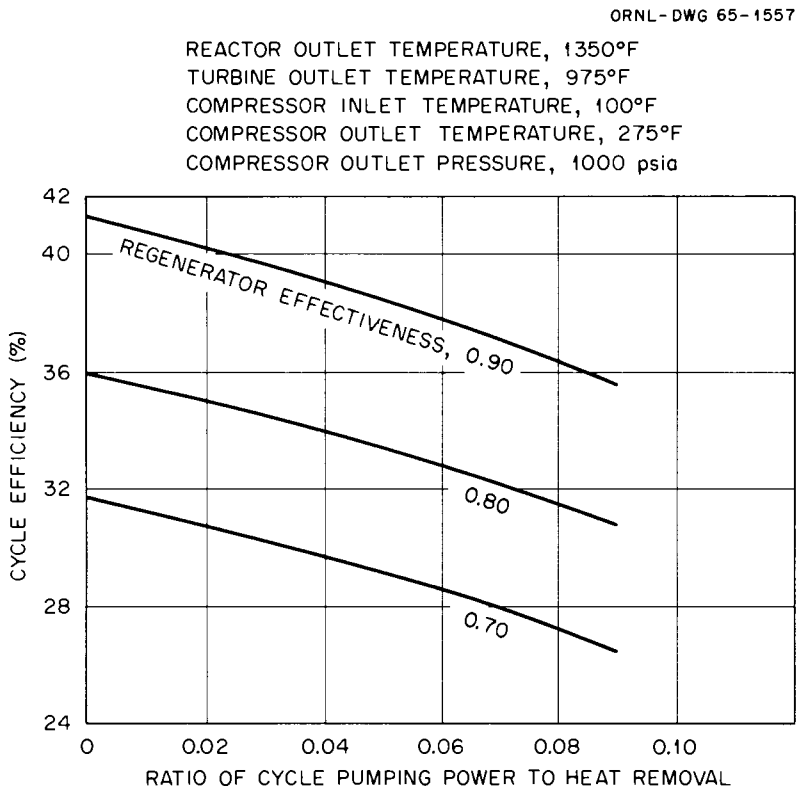

Fig. 5. Basic Cycle Efficiency as a Function of the Pumping Power-to-Heat Removal Ratio for CO_2, Assuming that It Is a Perfect Gas.

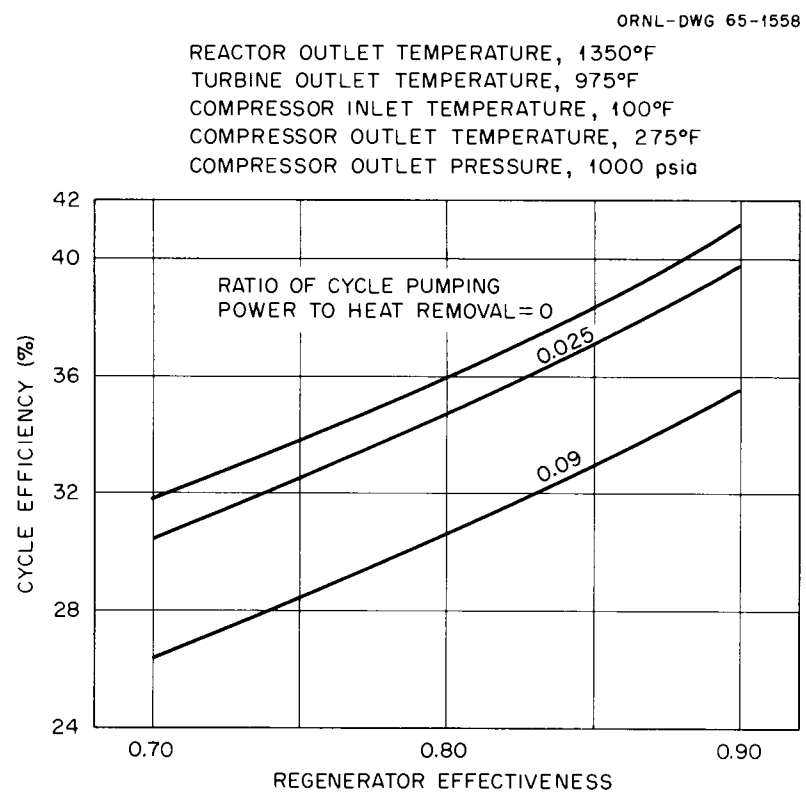

Fig. 6. Basic Cycle Efficiency as a Function of Regenerator Effectiveness for CO_2, Assuming that It Is a Perfect Gas.

ORNL-DWG 65-1559

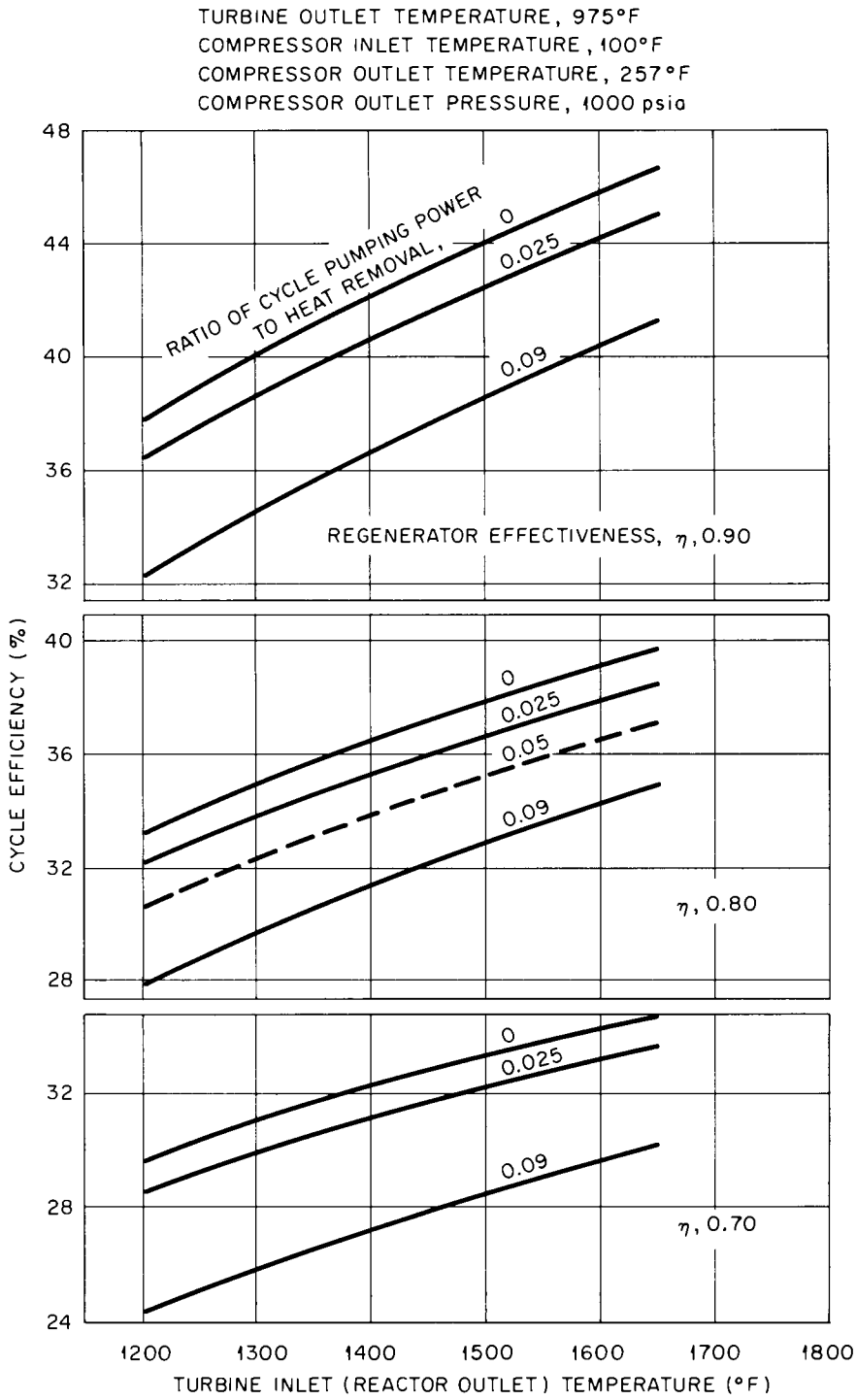

Fig. 7. Basic Cycle Efficiency as a Function of the Reactor Outlet Temperature for CO_2, Assuming that It Is a Perfect Gas.

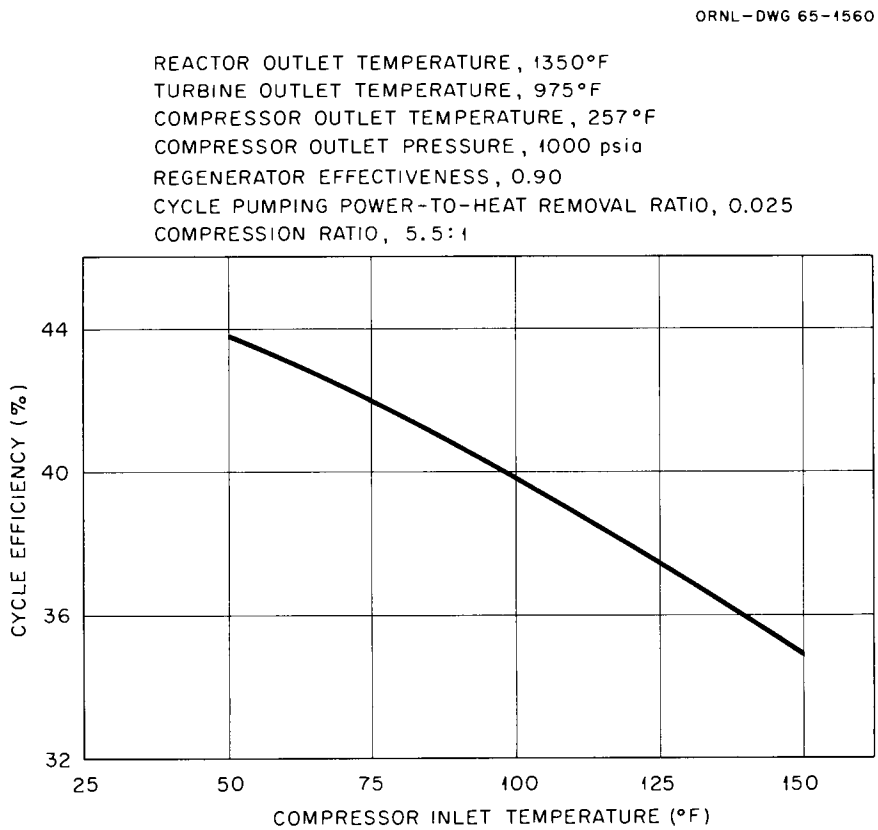

Fig. 8. Cycle Efficiency as a Function of the Compressor Inlet Temperature for CO_2, Assuming that It Is a Perfect Gas.

zero pumping power conditions, and it was about 7:1 for the 1650°F turbine inlet temperature, 70% regenerator effectiveness, and 0.09 pumping power-to-heat removal ratio condition. The compression ratio had a value between these limits for all the other cases investigated, and in no case in this region was the cycle efficiency very sensitive to the pressure ratio. Figure 9 shows the cycle efficiency versus the compression ratio for a typical case. It is apparent that for this case the cycle efficiency varies less than 0.5% in the compression ratio range from 5:1 to 7:1. A higher pumping power, a higher reactor outlet temperature, and a lower regenerator effectiveness will shift the peak of this curve toward a higher compression ratio. Thus the cycle efficiencies given in Figs. 5 through 8 correspond to near-optimum compression ratios. The pumping power-to-heat removal ratio referred to in these figures was the sum of those for the reactor, the regenerator, and the cooler, with

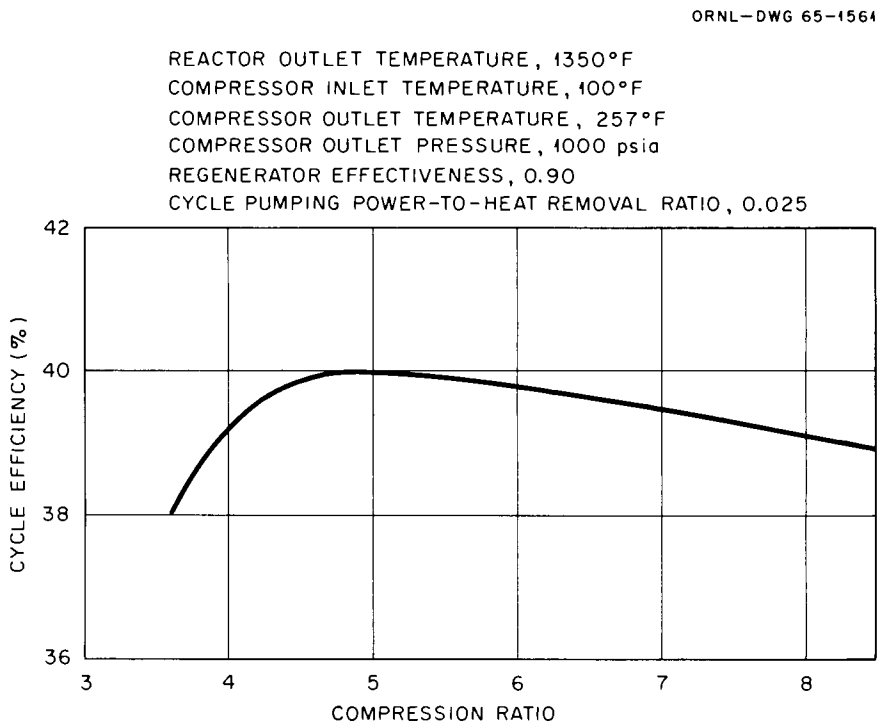

Fig. 9. Cycle Efficiency as a Function of the Compression Ratio for CO_2, Assuming that It Is a Perfect Gas.

the pumping power required for each duct divided equally between the units at either end of the duct.

The procedure for evaluating the cycle efficiency is explained in Appendix A. In these calculations, CO_2 was treated as a perfect gas, and its enthalpy was obtained from the gas tables.[7] The compression process for CO_2 in the high-pressure compressor takes place near enough to the saturation region so that deviations from the ideal perfect gas relations are appreciable and influence the calculations for the cycle efficiency. Calculations on the IBM computer, which took into account variations in the specific heat with pressure in the region near saturation, gave cycle efficiencies 2 to 3% lower than the initial calculations that were made assuming the perfect gas relations.

Effects of Regenerator Design on Cycle Performance and Costs

Many gas-turbine performance studies give a misleading impression of the effects of the amount of regeneration on overall cycle performance

and cost because they do not fully take into account the effects of increased regenerator size on both pumping power losses and regenerator capital charges as the regenerator effectiveness is increased. A substantial portion of the work of this study was concerned with these and related effects.

Effects of Heat Exchanger Proportions on Costs

An extensive study of steam generators for gas-cooled reactor applications was carried out in connection with an overall series of gas-cooled reactor studies and was reported previously.[8] This work indicated that the most promising heat transfer matrix for the steam generators is one employing 0.5-in.-OD, 0.4-in.-ID bare tubes arranged with their axes parallel to the axis of a cylindrical shell. This arrangement is well suited to the regenerator for a gas-turbine system if the high-pressure high-density gas from the compressor is passed through the inside of the tubes while the low-pressure, low-density hot gas from the turbine inlet is passed between the tubes. This at once maximizes the tube spacing in the header sheets and minimizes the pressure acting on the shell and hence the weight and cost of the shell. Further, the tubes will not tend to collapse under external pressure because of creep buckling.

Another investigation showed that the flow area outside the tubes should be about three times that inside the tubes because of the large difference in density between the two regions. This factor of 3 gives a nearly optimum set of proportions and falls in a range where the characteristics are insensitive to moderate changes in the area ratio. A similar tube-and-shell configuration was used for the cooler, with the cooling water flowing inside the tubes and the gas outside the tubes. It is reassuring to note that a completely independent study at General Atomic[4] had previously led to essentially the same conclusions, further indicating the soundness of this choice of heat transfer matrix.

Analytical expressions for the relationships between the pumping power-to-heat removal ratio, the gas mass flow rate inside the tubes, the tube length, and the gas temperature rise through the regenerator were worked out as shown in Appendix B. Similar expressions were derived for

the coolers in Appendix C. These expressions were used to construct the charts shown in Figs. 10 and 11. Figure 10 gives the tube length and the pumping power-to-heat removal ratio as a function of the mass flow rate of the gas inside the tube for each different gas temperature rise in

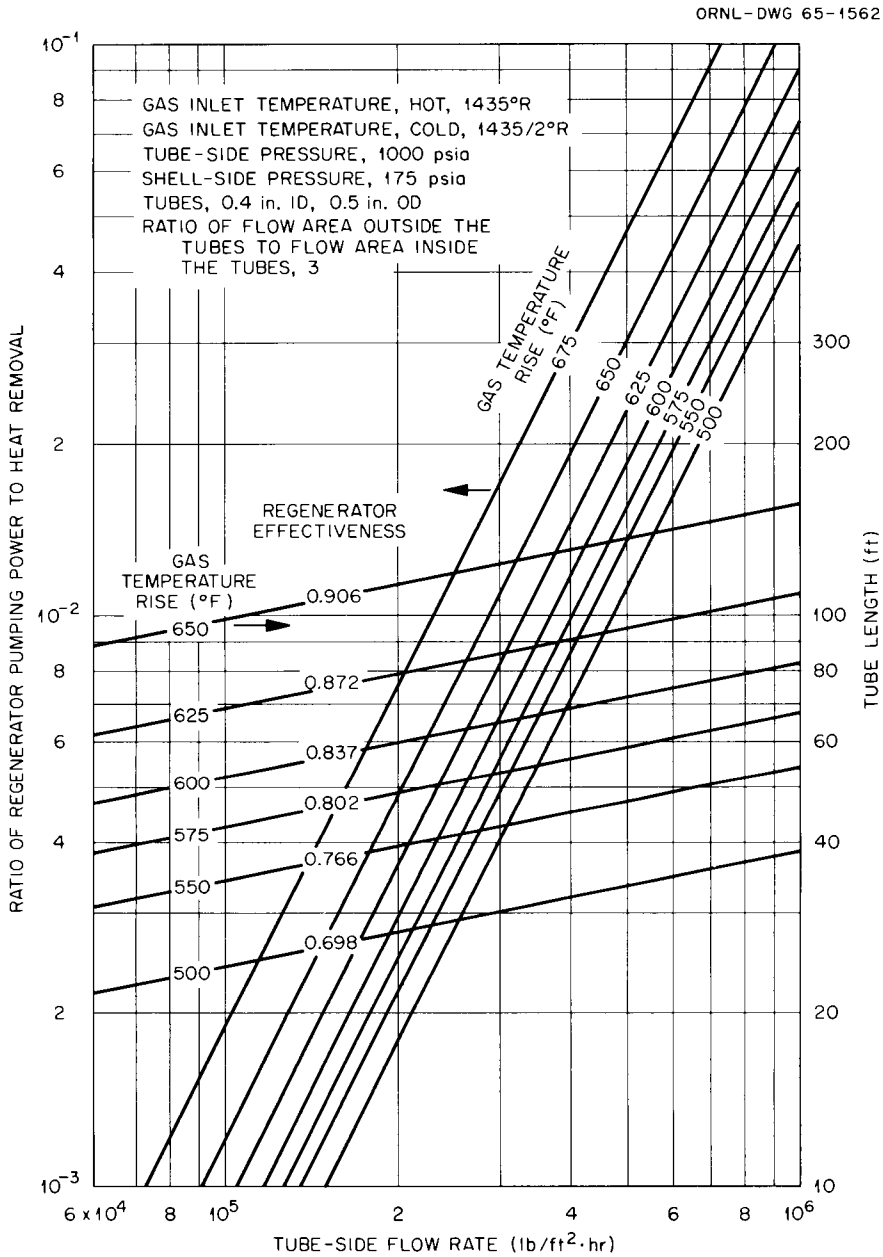

Fig. 10. Pumping Power-to-Heat Removal Ratio and Tube Length as Functions of Mass Flow Rate for Tube-and-Shell Regenerators Operating with CO_2.

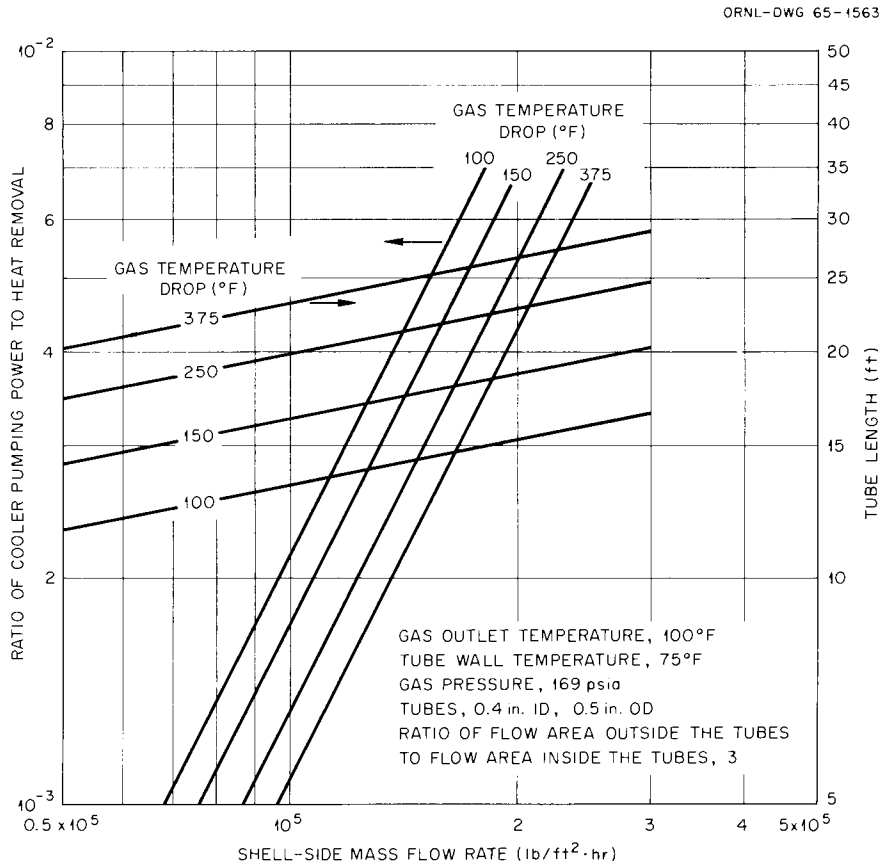

Fig. 11. Pumping Power-to-Heat Removal Ratio and Tube Length as Functions of the Shell-Side CO_2 Flow Rate Through the Cooler.

the regenerator for the conditions specified in the figure. Equations (B.15) and (B.17) were used in constructing the curves for the pumping power-to-heat removal ratio, and Eq. (B.34) was used in constructing the curves for the tube length. In these calculations the effects of tube wall thickness were neglected; that is, a value of unity was assumed for the ratio of the outside to the inside area of the tube. Figure 11 gives the tube length and the pumping power-to-heat removal ratio for the cooler as a function of the gas mass flow rate outside the cooler tubes. Equations (C.8) and (C.19) were used in constructing this chart. Figure 12 (constructed by using data from Figs. 10 and 11) gives the values of the B factor used in determining the tube surface area as a function of pumping power-to-heat removal ratio for the different values of gas temperature rise. The total heat transfer surface area for the heat exchanger,

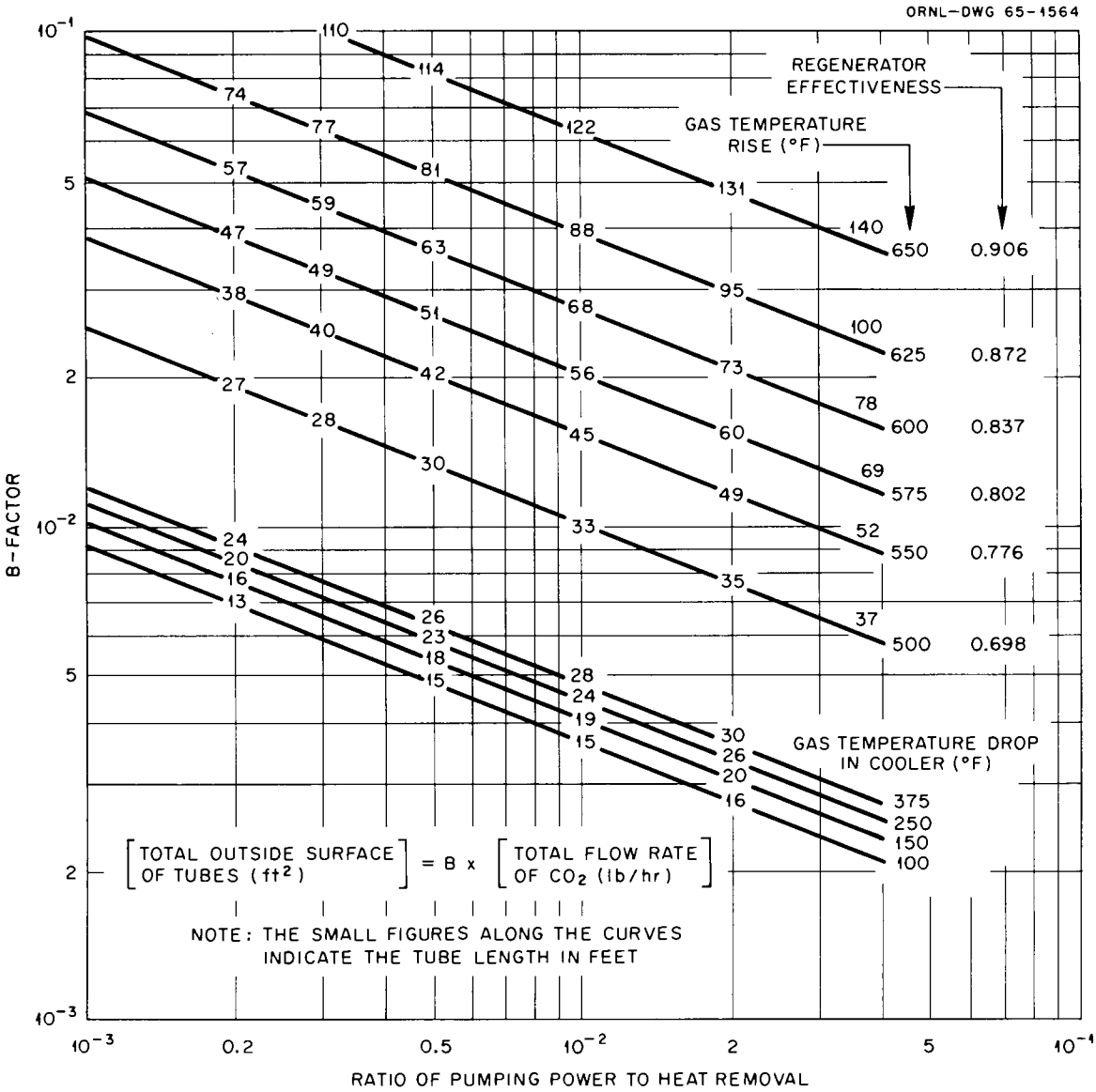

Fig. 12. B-Factors To Be Used in Evaluating Total Heat Transfer Area of the Coolers and Regenerators of Figs. 10 and 11.

based on the external tube surface, can easily be obtained by multiplying the B factor by the total mass flow rate of CO_2 in pounds per hour. The corresponding tube lengths are also indicated in Fig. 12. The derivation of the B factor is explained in Appendix D. Charts such as these are indispensable to an expeditious calculation, since they give direct, explicit solutions to problems that otherwise would have to be solved by using an

implicit analytical expression that would require several iterations to obtain an acceptable approximation for each case of interest.

Having established relations between the pumping power-to-heat removal ratio, the regenerator gas temperature rise, the mass flow rate, and the tube length, the next problem was to establish the size and cost of the heat exchanger units. The most promising way to build these is to run the tubes into nearly conventional header sheets. While flat header sheets would be simplest, at the high pressures and temperatures desired for these units, a maximum header sheet thickness of 10 in. would limit the diameter of a flat header sheet to perhaps 2 ft. This would make it necessary to use a large number of small-diameter headers and would introduce a major problem in manifolding the ducts into and out of the many small regenerator units. Previous work on heat exchangers in which excessive header sheet thicknesses have been a problem (e.g., steam boilers) has indicated that the best procedure is to make use of cylindrical or spherical headers so that bending stresses are eliminated. Spherical header sheets appear to be more suitable for this application. Analytical work has shown that the stress concentrations associated with the tube penetrations through the header require that the header sheet thickness in the vicinity of the penetrations be approximately three times that for an unperforated vessel of the same size and shape.[9] The maximum header sheet thickness practicable was considered to be 10 in. This gave a maximum radius of 4.15 ft. Previous experience with heat exchanger headers for the molten-salt aircraft reactor indicated that the penetrations in well-proportioned cylindrical or spherical headers should not deviate more than about 30° from the radial direction, so the maximum diameter of the circle enclosing the perforated region becomes 7.2 ft if the holes in the header sheet are to be parallel.

In estimating the weight and cost of the shells, the bulk of the rest of the spherical vessel serving as the header was assumed to have a thickness 30% of that in the thickened zone in the tube penetration region (except in the vicinity of duct penetrations). It was assumed that those portions of the heat exchangers that would operate below 700°F would be fabricated of SA-212, grade B, carbon steel. For the balance of the system, where temperatures up to 970°F might be experienced, a

low chromium-molybdenum steel was assumed. The allowable stress for this material for 1% creep in 100,000 hr was taken as 10,000 psi.[10]

The differential expansion between the tubes and the shell arising from the temperature drop through the gas film on the tube would amount to approximately 3/8 in. in 100 ft for a typical heating effectiveness. While it would entail considerable complication, this temperature differential (and the associated differential expansion) could be reduced by arranging some spiral tubes around the outer perimeter of the bundle just inside the shell and providing baffles so that the shell would run at a temperature close to that of the hot gas from the turbine rather than close to the temperature of the gas from the compressor.

Several methods of accommodating differential thermal expansion between the tubes and the shell were considered. These included U-shaped shells similar to those in the Maritime gas-cooled reactor, a "hockey-stick" heat exchanger shell, and a floating-head arrangement. The first two did not lend themselves well to an overall power plant configuration. The floating-head arrangement might be satisfactory if a packed joint were employed at the cold end of the regenerator. However, this arrangement would place the tubes in compression and might lead to buckling. While unconventional, a more promising approach than any of these was suggested by the fact that the tubes are so long and slender that they will buckle elastically as columns. A brief analysis disclosed that this affords a sound basis for design. Prior to installation the tubes could be bent slightly between spacers so that they would all be predisposed to buckle in the same fashion, with a node at each spacer grid, and thus maintain a uniform tube spacing. This approach seemed to be particularly in order, since, for a high regenerator effectiveness, the temperature difference between the tube and the shell would be sufficiently small so that it could be accommodated elastically without buckling, except for unusual temperature transients.

Heat exchanger costs were estimated by summing the cost of the pressure vessel, the tubing, and the tube-to-header joints. The pressure vessel cost was calculated from the weight using the cost per pound given

by Fig. 11.1 of ref. 11. The tubing cost was taken as $0.50/ft for low-alloy steel. The cost of the tube-to-header joints was taken as $10 per tube. The joints were assumed to be rolled, not welded, since the degree of leaktightness required in the regenerator is not high. The value of $10 per tube was intended to include the cost of drilling the header sheets and the assembly work, including jigging, rolling the tubes into the header sheets, and installing spacers. While these basic cost factors are low, they might be attained if a large number of similar units were built. The sum of these three basic cost items does not include the cost of design, overhead, transportation, or erection, but these latter cost factors would probably be roughly proportional to the base cost as estimated here.

Effects of Turbine-Compressor Units on Costs

The turbine size was estimated using conventional techniques to scale up the output of commercial gas-turbine units designed for open-cycle operation with air as the working fluid. The power output was assumed to vary directly with the minimum gas density in the cycle, the square of the rotor diameter, and the square of the rotor tip speed. The compressibility limit on the rotor tip speed was taken as inversely proportional to the square root of the molecular weight of the gas and directly proportional to the square root of the turbine inlet absolute temperature. The stress limit on the tip speed was taken to be that implied by experience with units designed for use with air. It was found that a direct-drive, 3600-rpm turbine unit having a diameter of 5.3 ft and operating on CO_2 would serve to give an electrical output of 167 Mw. Since the proportions of this unit seemed reasonable, and since reliability considerations indicated that it would be desirable to have at least three turbine units in the plant, this size was chosen.

The cost of the turbine-generator units was extrapolated from the data available for 20,000-kw(e) units currently on the market. The cost of the turbine-compressor unit was assumed to be inversely proportional to the square root of the peak pressure in the system for a given size

of unit. The combined effects of these factors gave an estimated cost of $50/kw(e) for the units chosen.

Effects of Reactor Design Parameters on Fuel-Cycle Costs

As another of the series of studies of gas-cooled reactor systems, of which this report represents a part, an analysis was made of the effects of reactor design parameters on fuel-cycle costs[12] for both graphite- and BeO-moderated reactors. Figure 13 from this unpublished study shows a measure of the sum of the reactor capital charges* and the fuel-cycle cost† for a 500-Mw net electrical output, BeO-moderated, gas-cooled reactor specific power. The analysis assumed a second- or third-generation reactor based on a successful development program, and it neglected development costs. The estimate was made in mills per kilowatt-hour, but the values given on the curves are labeled "relative costs" to emphasize that there are no firm bases for some of the cost factors such as fabrication and reprocessing. A thermal efficiency of 40%, a beryllium-to-uranium ratio of 2000, and a void fraction of 0.25 were assumed for these calculations. The relative cost for thermal efficiencies other than 40% can be obtained by multiplying the data in Fig. 13 by the adjustment factors given in Fig. 14.

The effects of specific power on the relative costs for the fuel cycle alone for a thermal efficiency of 40% are shown in Fig. 15. By multiplying these data by the adjustment factors of Fig. 16, the fuel-cycle costs for cycle efficiencies other than 40% can be obtained. As one indication of the way in which specific power affects the reactor capital charges, the size of the pressure vessel for the 500-Mw(e), BeO-moderated reactor is shown in Fig. 17 as a function of the reactor specific power for different thermal efficiencies.

---

*Reactor capital charges include the material and fabrication costs of the pressure vessel and the moderator. They do not include design, overhead, contingency, etc.

†The fuel-cycle cost includes the cost of ^{235}U burned in the core, fuel element fabrication and material cost, capital charges for the fuel-handling equipment, the cost of fuel reprocessing, and interest on the fuel inventory less the fuel savings derived from conversion.

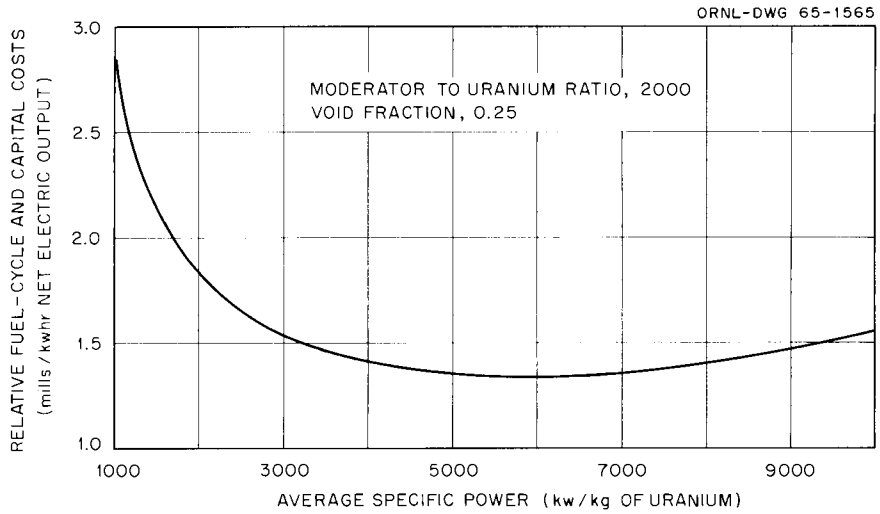

Fig. 13. Relative Reactor Capital and Fuel-Cycle Costs for a Thermal Efficiency of 40%.

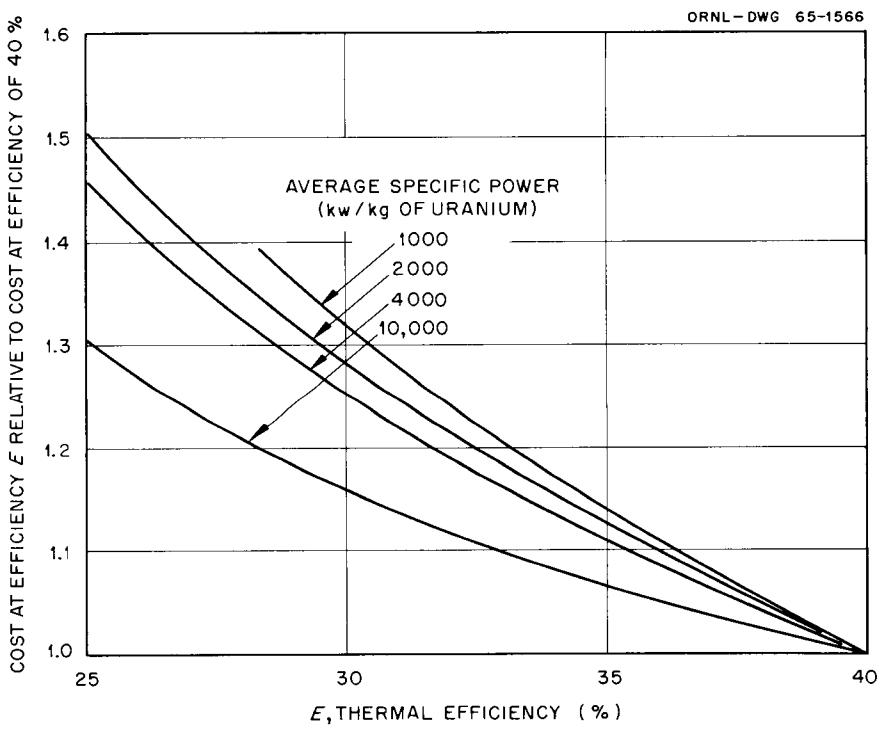

Fig. 14. Factors for Adjusting Data of Fig. 13 to Other Cycle Efficiencies.

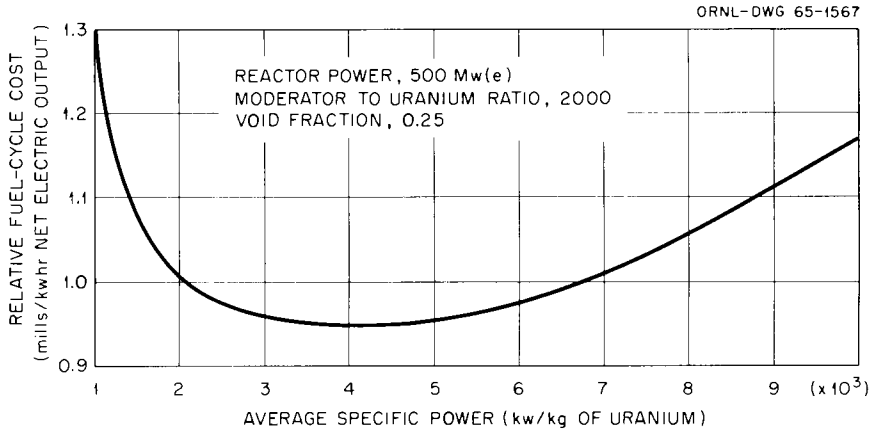

Fig. 15. Relative Fuel-Cycle Cost for a Thermal Efficiency of 40%.

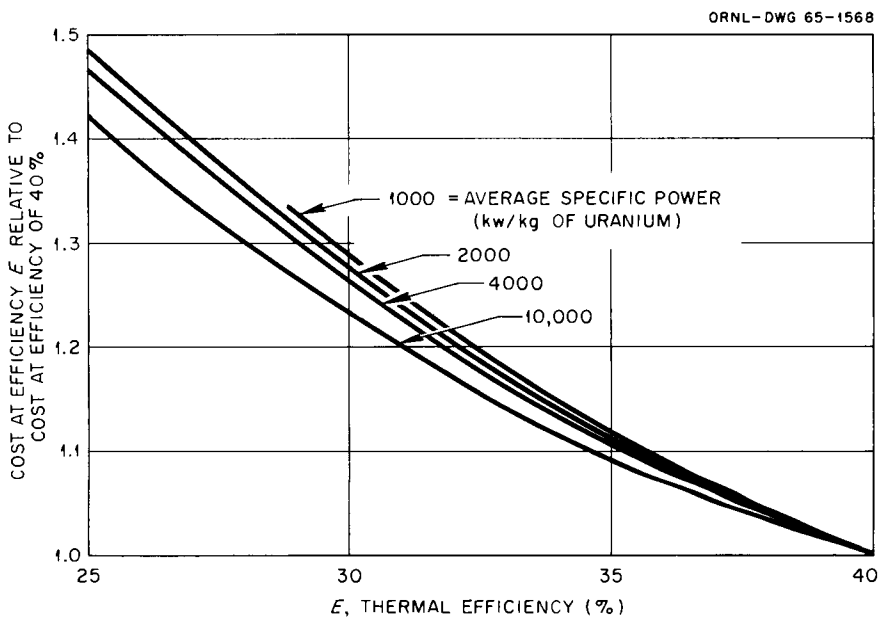

Fig. 16. Factors for Adjusting Data of Fig. 15 to Other Cycle Efficiencies.

It is apparent from Fig. 13 that the sum of the fuel-cycle costs and the reactor capital charges drops off rapidly as the reactor specific power is increased to about 3000 kw/kg of uranium, or to an average core power density of about 27 kw/liter of core. A further increase in reactor specific power changes the cost only a little up to about 6000 kw/kg, but fuel element thermal stress considerations impose an upper limit on the

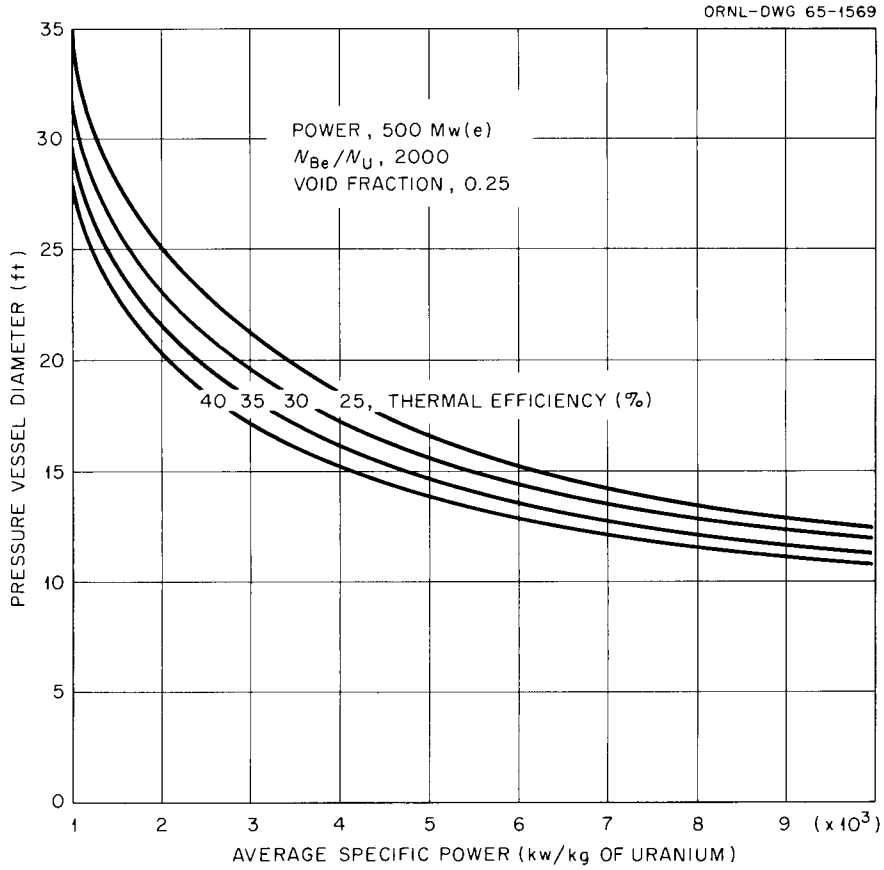

Fig. 17. Pressure Vessel Diameter as a Function of Average Specific Power.

reactor specific power. In selecting a set of core design parameters for the tubular $BeO-UO_2$ fuel elements* considered, it was assumed that the fuel element power density would be limited to about 600 watts/cm^3 of fuel element by thermal stress considerations. If allowances are made for the difference in power density between the fuel element and the core as a whole and for nonuniformities in the core power density, the corresponding average core power density would be about 36 kw/liter for the

*The fuel elements were taken as 7/8-in.-OD, 5/8-in.-ID tubes 12 in. long with a cross-sectional area of 0.22 in.^{2}, a channel gross cross-sectional area of 1.13 in.^{2}, an hexagonal-block gross cross-sectional area of 3.65 in.^{2}, and a distance across the flats of the hexagonal moderator blocks of 2.05 in.

core, or the average reactor specific power would be 4000 kw/kg of uranium.

The effects of these parameters on a helium-cooled graphite reactor are similar. Figure 18 shows the relative reactor capital cost and the fuel-cycle cost as a function of the cycle efficiency for a graphite-moderated, helium-cooled reactor for the conditions specified on the figure. The average power density in the core as a whole was about 40 watts/cm^3. It is to be noted that, for a 500-Mw net electrical output, the lower thermal efficiency of a gas-turbine plant leads to a larger diameter reactor than for a steam-turbine plant if the power density is the same in both cases.

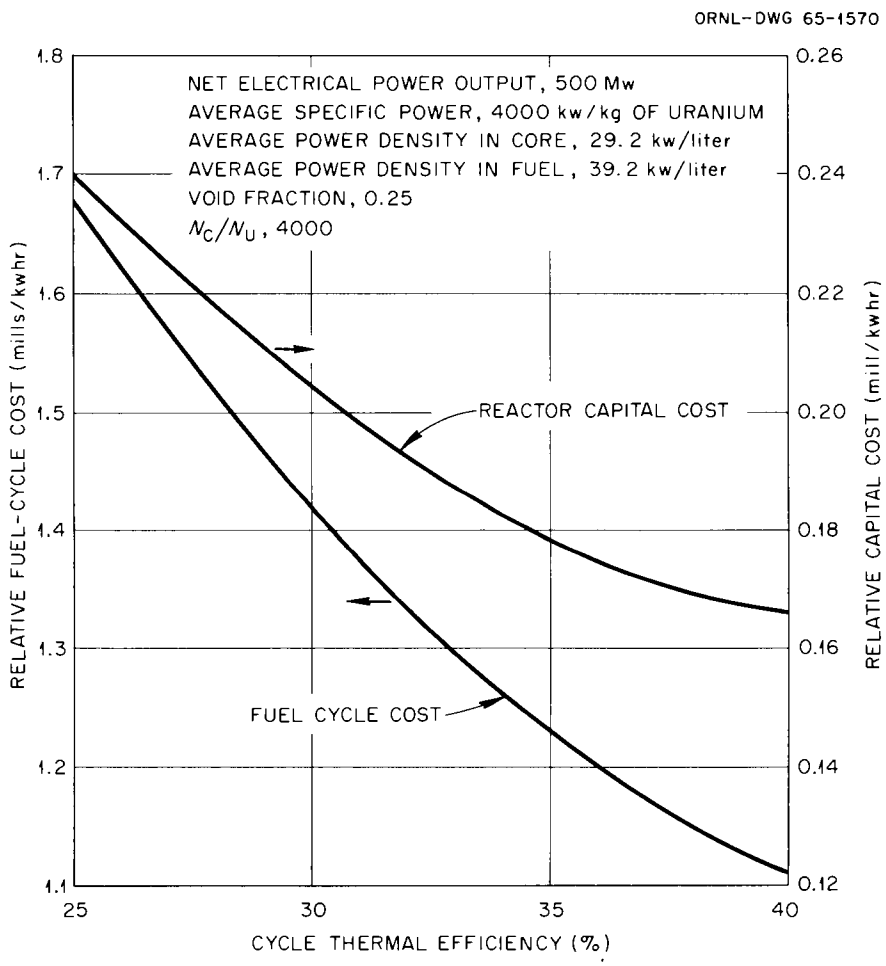

Fig. 18. Effect of Cycle Efficiency on the Capital Cost and Fuel-Cycle Cost of Graphite-Moderated Helium-Cooled Reactors with Unclad Fuel Elements.

Effects of Pressure Losses and Regenerator Effectiveness on Costs

In applying the generalized cycle efficiency, design, and cost data of the preceding sections to arrive at a well-proportioned plant design, it appeared that the first step should be to provide a basis for choosing a regenerator effectiveness and values for the major pressure losses. To do this, the effects of the regenerator effectiveness and system pressure losses on costs were investigated. It is evident that increasing the pumping power reduces the cycle efficiency and thus increases the fuel costs, but it reduces the capital charges. Increasing the regenerator effectiveness, on the other hand, improves the cycle efficiency and thus reduces the fuel costs, but it increases the regenerator capital charges. Further, the distribution of pumping power among the different units in the cycle is also important. If too little pumping power were allowed for gas flow through the ducts, the ducts would become excessively large, while the regenerator or reactor capital charges would be excessive if the pumping power allowed for these components were too small.

The effects of the above parameters on the cost of a 500-Mw net electrical output gas-cooled reactor and gas-turbine plant were investigated. A 1000-psia CO_2 cycle with 1350°F turbine inlet, 975°F turbine outlet, 100°F compressor inlet, and 257°F high-pressure compressor outlet conditions was selected for the reference cycle. A BeO-moderated reactor operating at a specific power of 4000 kw/kg of uranium was assumed.* The regenerator and the cooler were the same as those described previously. The capital charges and the fuel-cycle cost for such a power plant were calculated for regenerator effectivenesses of 70, 80, and 90% and pumping power-to-heat removal ratios of 0.025, 0.05, and 0.09 for the cycle. The distribution of pumping power in the above cycles was made such that the pumping power-to-heat removal ratios for the regenerator were 0.01, 0.02, and 0.04, respectively. A pumping power-to-heat removal ratio of 0.005 was allowed for the cooler in all cases. The balance of the pumping power

*As is apparent from Fig. 13, if thermal stresses in the fuel elements made it necessary to reduce the specific power to 3000 kw/kg of uranium, the fuel cost would increase by only about 0.15 mill/kwhr.

in each case was assumed to go into pumping the gas through the rest of the cycle.

Table 2 shows the resulting costs for the reactor, the regenerator, the cooler, the turbine, and the compressors. For convenience in the calculations, the shell diameters for the regenerator and cooler units were fixed, but the number and the lengths of these units were allowed to vary depending on the conditions selected. The shell thickness in each case was based on a 360-psia system gas pressure. (Although the gas pressure for the shell side of the cooler and the regenerator would be only about 180 psia during normal reactor operation, it would be essential that the shell withstand the 360-psia condition that would prevail immediately following an abrupt shutdown.) The hot gas would enter the generator shell at 975°F and leave at a temperature of 300 to 350°F. Thus the allowable stress is lower at the high-temperature end of the shell than at the low-temperature end. For convenience in the calculations, an allowable stress of 10,000 psia was assumed for the hot end of the regenerator shell and 16,000 psia for the cold end. An allowable stress of 16,000 psia was assumed for the cooler.

Figures 19 through 22 show the results of these calculations. Figure 19 gives the reactor capital charges and the fuel-cycle cost (definitions of these cost terms as used here were given earlier in the text) in mills per kilowatt-hour of net electrical output as a function of the regenerator effectiveness for different values of the pumping power-to-heat removal ratio. Figure 20 gives costs for the regenerator and the cooler, and Fig. 21 gives the sum of the reactor capital charges and the fuel cycle, regenerator, and cooler costs as functions of regenerator effectiveness.

The cost of the turbine-compressor unit was assumed to be $50/kw(e). A total allowable pumping power-to-heat removal ratio of 0.05 and a regenerator effectiveness of 0.80 were assumed for the cycle. Assuming 14% fixed charges and 6000 hr of full-power operation per year, the power cost equivalent of the turbine and compressor cost was 1.165 mills/kwhr net electrical output. The cost of the turbine-compressor unit for other cycle conditions was taken as directly proportional to the total mass flow rate of the gas for the cycle.

Table 2. Effects of Pumping Power-to-Heat Removal Ratio and Regenerator Effectiveness on the Cost of a 500-Mw(e) Direct-Cycle BeO-Moderated CO_2-Cooled Gas-Turbine Power Plant

Reactor specific power: 4000 kw/kg of uranium
Core voidage: 0.25
Reactor gas outlet temperature: 1350°F
Turbine gas inlet temperature: 1350°F
Turbine gas outlet temperature: 975°F
Compressor inlet temperature: 100°F

Compressor outlet temperature: 257°F
Compressor pressure: 1000 psia
Regenerator and cooler tubes: 0.4 in. ID, 0.5 in. OD
Ratio of flow area outside tubes to flow area inside tubes: 3
Operation: 6000 hr per year

		1	2	3	4	5	6	7	8	9
1	Regenerator effectiveness	0.90	0.90	0.90	0.80	0.80	0.80	0.70	0.70	0.70
2	Ratio of total pumping power to heat removal from reactor for the cycle	0.025	0.05	0.09	0.025	0.05	0.09	0.025	0.05	0.09
3	Ratio of regenerator pumping power to heat removal	0.01	0.02	0.04	0.01	0.02	0.04	0.01	0.02	0.04
4	Ratio of cooler pumping power to heat removal	0.005	0.005	0.005	0.005	0.005	0.005	0.005	0.005	0.005
5	Gas temperature rise in reactor, δt_r, °F	447.5	447.5	447.5	518.5	518.5	518.5	590.5	590.5	590.5
6	Gas temperature rise in regenerator, δt_{reg}, °F	645	645	645	574	574	574	502	502	502
7	Gas temperature drop in cooler, δt_{cooler}, °F	230	230	230	301	301	301	363	363	363
8	Compression ratio	5.54		6.41	5.56		6.55	5.60		6.68
9	Basic cycle efficiency (from Fig. 5)	0.399	0.382	0.356	0.347	0.332	0.306	0.305	0.290	0.264
9a	Net cycle efficiency, E = basic cycle efficiency − 0.025	0.374	0.375	0.331	0.322	0.307	0.281	0.280	0.265	0.239
	Reactor									
10	Reactor capital and fuel-cycle cost (from Figs. 13 and 14), mills/kwhr	1.490	1.540	1.660	1.680	1.745	1.870	1.895	1.965	2.130
11	Reactor fuel-cycle cost (from Figs. 15 and 16), mills/kwhr	0.995	1.025	1.095	1.125	1.172	1.265	1.270	1.325	1.460
12	Reactor capital cost = /10/ − /11/, mill/kwhr	0.495	0.515	0.565	0.555	0.573	0.605	0.625	0.640	0.690
13	Reactor pressure vessel diameter (from Fig. 17), ft	15.6	15.9	16.4	16.7	17.0	17.5	17.6	18.2	19.0
14	Total CO_2 flow in the cycle = (500,000 × 3413)/($Ec_p\ \delta t_R$), lb/hr	35.1×10^6	36.8×10^6	39.7×10^6	35.6×10^6	37.5×10^6	40.8×10^6	35.8×10^6	38.6×10^6	42.2×10^6
14a	Specific heat of CO_2 in reactor, Btu/lb·°F	0.290	0.290	0.290	0.288	0.288	0.288	0.286	0.286	0.286
	Regenerators									
15	Total heat transfer area for regenerators (from Fig. 12), ft^2	21.0×10^5	16.1×10^5	13.8×10^5	7.1×10^5	5.6×10^5	4.7×10^5	3.65×10^5	3.03×10^5	2.56×10^5
16	Length of regenerator tube (from Fig. 12), ft	117	125	134	56	60	64	33	35	38
17	Total number of regenerator tubes = n = area/πDL = $7.63 \times$ /15//16/, ft	1.37×10^5	0.985×10^5	0.79×10^5	0.965×10^5	0.711×10^5	0.560×10^5	0.845×10^5	0.661×10^5	0.515×10^5
18	Total length of regenerator tubes = nL = /17/ × /16/, ft	16.05×10^6	12.3×10^6	10.58×10^6	5.40×10^6	4.26×10^6	3.58×10^6	2.89×10^6	2.31×10^6	1.96×10^6
19	Total cost of regenerator tubes (at $10/tube + $0.50/ft)	9.37×10^6	7.13×10^6	6.08×10^6	3.67×10^6	2.84×10^6	2.35×10^6	2.29×10^6	1.72×10^6	1.50×10^6
20	Total cross-sectional area of regenerators = $n(\pi/4) \times [3(0.4/12)^2 + (0.5/12)^2]$ = /17/251, ft^2	545	392	314	383	283	223	336	263	205
21	Number of regenerators (assume 7.2-ft-diam cylindrical shells)	13.6	9.8	7.8	9.6	7.1	5.6	8.4	6.6	5.1
22	Weight of headers for one regenerator = $2[3/4 \times 2.5/12) + (1/4 \times 10/12)]\ \pi \times (100/12)^2 \times 500$, lb	79.6×10^3	79.6×10^3	79.6×10^3	79.6×10^3	79.6×10^3	79.6×10^3	79.6×10^3	79.6×10^3	79.6×10^3
23	Weight of shell for one regenerator = $\pi \times 7.2 \times (1.7 + 1.1)/(2 \times 12) \times L \times 500 = 1315 \times$ /16/, lb	154.0×10^3	164.5×10^3	176.5×10^3	73.8×10^3	79.0×10^3	84.3×10^3	83.5×10^3	46.1×10^3	50.0×10^3
24	Total cost of shells and headers for all regenerators (at $3/lb for headers and $1/lb for shell)	5.35×10^6	3.95×10^6	3.23×10^6	3.00×10^6	2.25×10^6	1.81×10^6	2.38×10^6	1.88×10^6	1.48×10^6
25	Total cost of regenerator = /19/ + /24/, $	14.72×10^6	11.08×10^6	9.31×10^6	6.67×10^6	5.09×10^6	4.16×10^6	4.67×10^6	3.60×10^6	2.98×10^6
26	Total cost of regenerator = (/25/ × 1000 × 0.14)/(500,000 × 6000) = /25/ × 0.0467 × 10^{-6}, mill/kwhr net	0.688	0.516	0.436	0.313	0.238	0.195	0.218	0.168	0.140

Table 2. (continued)

		1	2	3	4	5	6	7	8	9
	Coolers									
27	Total heat transfer area for coolers (from Fig. 12), ft^2	2.00×10^5	2.09×10^5	2.26×10^5	2.13×10^5	2.22×10^5	2.44×10^5	2.22×10^5	2.49×10^5	2.61×10^5
28	Length of cooler tube (from Fig. 12), ft	22	22	22	24	24	24	26	26	26
29	Total number of cooler tubes = area/πDL = 7.63 × /27/ / /28/	69.2×10^3	72.5×10^3	78.5×10^3	67.8×10^3	70.6×10^3	77.5×10^3	65.2×10^3	73.0×10^3	76.5×10^3
30	Total length of cooler tubes = /28/ × /29/, ft	1.52×10^6	1.59×10^6	1.73×10^6	1.63×10^6	1.70×10^6	1.86×10^6	1.69×10^6	1.89×10^6	1.99×10^6
31	Total cost of cooler tubes (at \$10/tube + \$0.50/lb)	1.433×10^6	1.479×10^6	1.651×10^6	1.493×10^6	1.556×10^6	1.705×10^6	1.497×10^6	1.675×10^6	1.760×10^6
32	Total cross-sectional area of coolers = $n(\pi/4)[3(0.4/12)^2 + (0.5/12)^2]$ = /29/251, ft^2	276	289	313	270	282	309	260	291	305
33	Number of coolers (assume 7.2-ft-diam cylindrical shell)	6.9	7.3	7.8	6.8	7.1	7.7	6.5	7.3	7.6
34	Weight of headers for one cooler = $2[(3/4 \times 0.6/12) + (1/4 \times 2.4/12)]\ \pi\ (100/12)^2 \times 500$, lb	18.1×10^3	18.1×10^3	18.1×10^3	18.1×10^3	18.1×10^3	18.1×10^3	18.1×10^3	18.1×10^3	18.1×10^3
35	Weight of shell for one cooler = $\pi D\ (1.1/12)\ L \times 500$ = 1045 × /28/, lb	23.0×10^3	23.0×10^3	23.0×10^3	25.1×10^3	25.1×10^3	25.1×10^3	27.2×10^3	27.2×10^3	27.2×10^3
36	Total cost of shell and headers for all coolers (at \$1.0/lb)	0.284×10^6	0.300×10^6	0.320×10^6	0.293×10^6	0.306×10^6	0.332×10^6	0.294×10^6	0.330×10^6	0.344×10^6
37	Total cost of coolers = /31/ + /36/, \$	1.427×10^6	1.779×10^6	1.971×10^6	1.786×10^6	1.862×10^6	2.037×10^6	1.791×10^6	2.005×10^6	2.104×10^6
38	Total cost of coolers = (/37/ × 1000 × 0.14)/(500,000 × 6000) = /37/ × 0.0467 × 10^6, mill/kwhr net	0.067	0.083	0.092	0.083	0.087	0.095	0.084	0.094	0.099
	Turbine and Compressors									
40	Turbine and compressor cost for case No. 5, \$/kw(e)					50[a]				
41	Turbine and compressor cost,[b] mills/kwhr net	1.091	1.145	1.203	1.111	1.165	1.270	1.115	1.200	1.310
	Summary of Costs									
42	Reactor fuel cycle, /11/, mills/kwhr net	0.995	1.025	1.095	1.125	1.172	1.265	1.270	1.325	1.440
43	Reactor capital cost, /12/, mill/kwhr net	0.495	0.515	0.565	0.555	0.573	0.605	0.625	0.640	0.690
44	Regenerator cost, /26/, mill/kwhr net	0.688	0.516	0.436	0.313	0.238	0.195	0.218	0.168	0.140
45	Cooler cost, /38/, mill/kwhr net	0.067	0.083	0.092	0.083	0.087	0.095	0.084	0.094	0.099
	Summary of Costs									
46	Reactor and heat exchanger costs, /42/ + /43/ + /45/, mills/kwhr net	2.245	2.139	2.088	2.075	2.070	2.160	2.197	2.227	2.369
47	Reactor, heat exchanger, and turbine-compressor costs, /41/ + /42/ + /43/ + /44/ + /45/, mills/kwhr net	3.336	3.284	3.292	3.187	3.235	3.430	3.312	3.427	3.679

[a] Turbine and compressor cost for case No. 5 = $\frac{1}{0.61}\left(\frac{\text{Max pressure for air unit}}{\text{Max pressure for } CO_2 \text{ unit}}\right)^{1/2} \times (\text{cost of air unit}) = \frac{1}{0.61}\left(\frac{90}{980}\right)^{1/2} \times 100$.

[b] Turbine and compressor cost = $\frac{50 \times 1000 \times 0.14}{6000} \times \frac{CO_2 \text{ flow rate}}{CO_2 \text{ flow rate for case No. 5}} = 1.165\ \frac{CO_2 \text{ flow rate}}{CO_2 \text{ flow rate for case No. 5}}$.

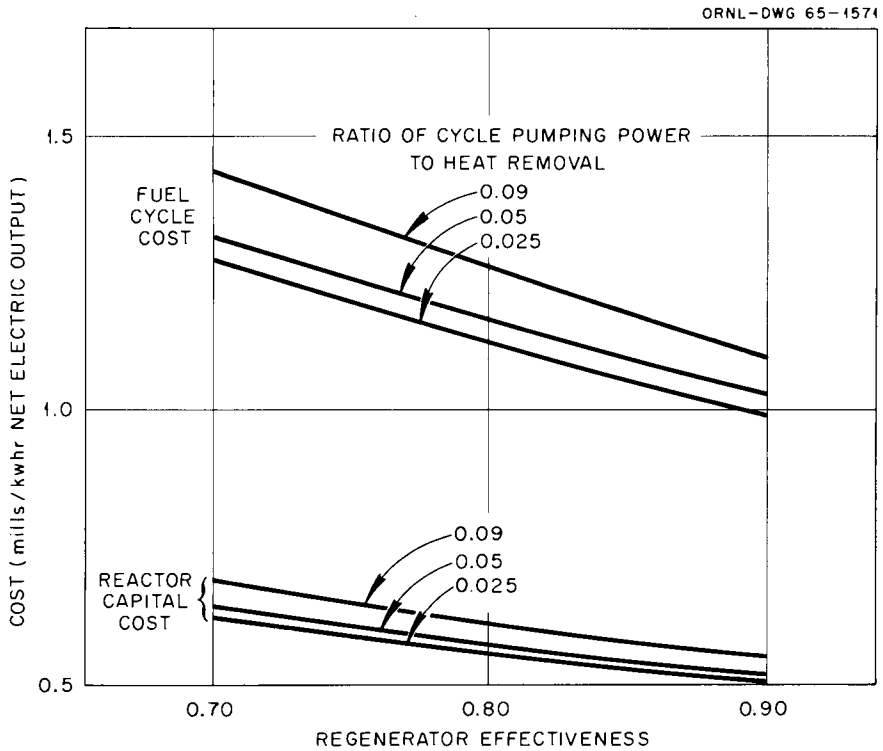

Fig. 19. Reactor Capital Charges and Fuel-Cycle Costs.

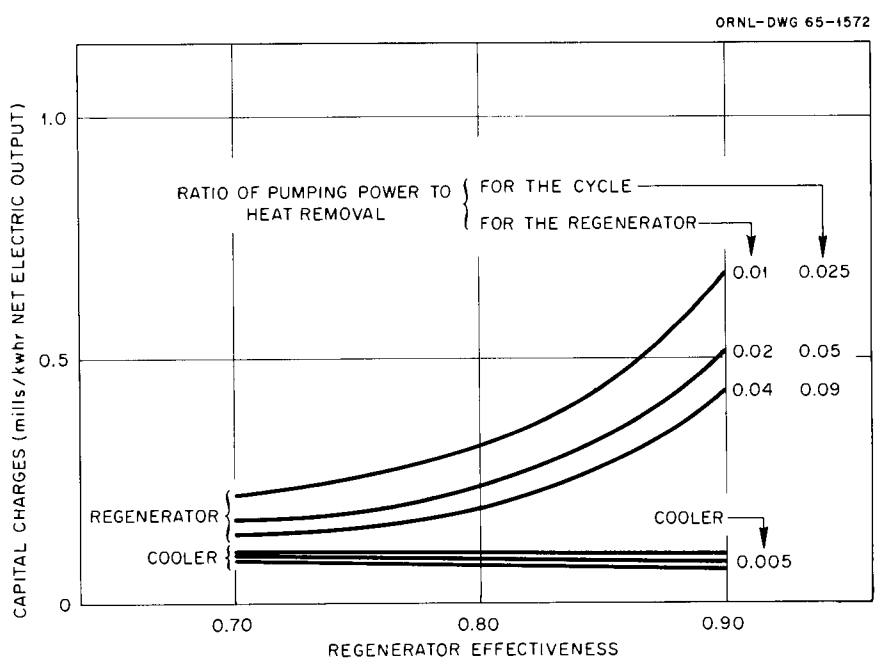

Fig. 20. Regenerator and Cooler Capital Charges.

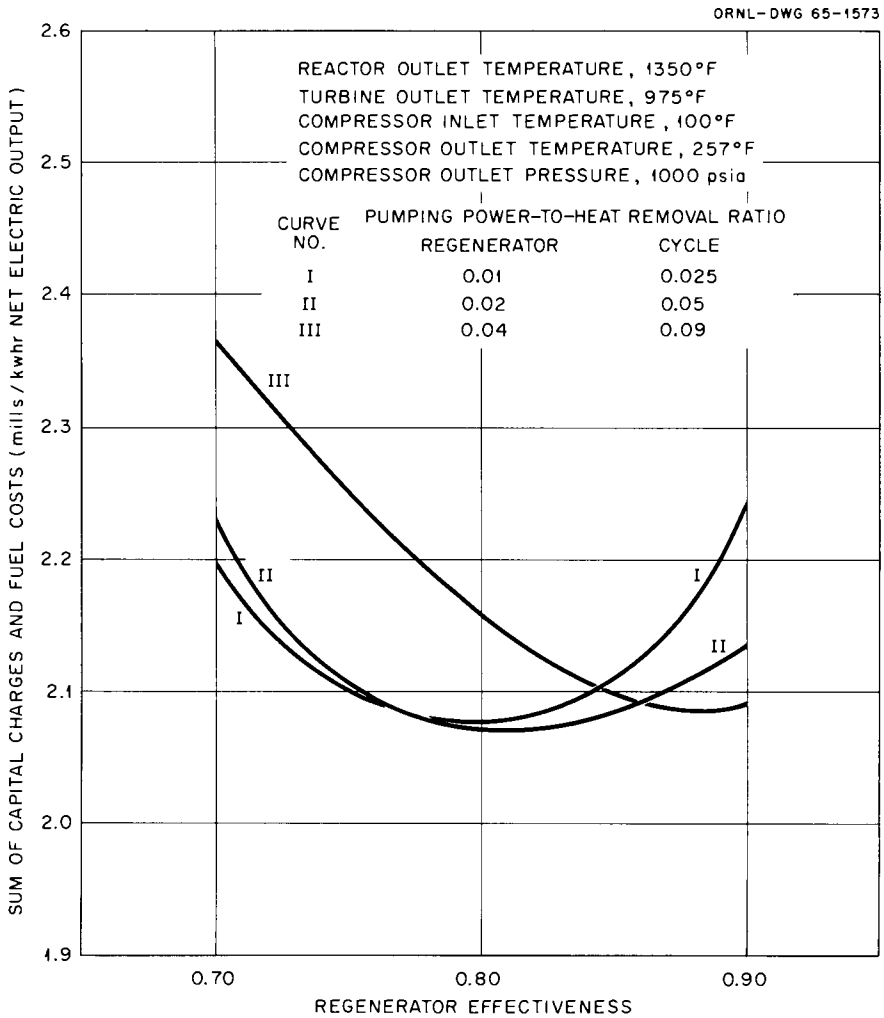

Fig. 21. Sum of Reactor Capital Charges and Fuel-Cycle, Regenerator, and Cooler Costs for Reference Reactor.

Figure 22 was obtained by adding the turbine-compressor unit cost calculated in this manner to the costs in Fig. 21. Therefore, Fig. 22 gives the sum of the reactor capital charges and the fuel-cycle, regenerator, cooler, and turbine-compressor unit costs as a function of the regenerator effectiveness for the different pumping power-to-heat removal ratios. It is apparent from this figure that the conditions of curves I and II yield a minimum cost for a regenerator effectiveness between 0.80 and 0.85 and that the curves are flat in this region. Although curve I gives the lowest cost, it allows a pumping power-to-heat removal ratio of only 0.015 for the entire cycle, excluding the regenerator. This low

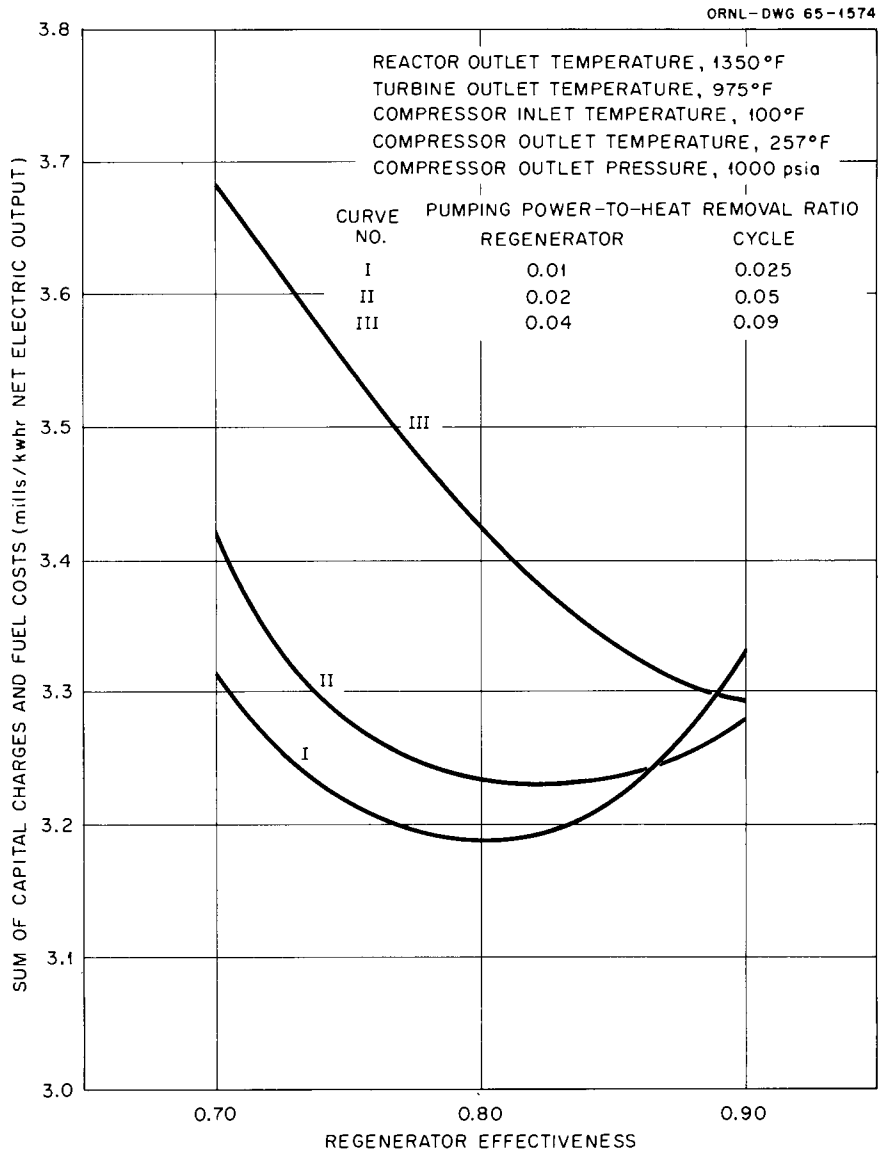

Fig. 22. Sum of Reactor Capital Charges and Fuel-Cycle, Regenerator Cooler, Turbine, and Compressor Costs for Reference Reactor.

figure would require unreasonably large ducts, and these would entail large capital charges. On the other hand, curve II not only gives reasonable costs for the components other than the ducts but allows a pumping power-to-heat removal ratio of 0.03 for the rest of the cycle, except the regenerator. As will be shown later, this value gives well-proportioned ducts. Curve III allows a pumping power-to-heat removal ratio of about 0.04 for the rest of the cycle, excluding the regenerator, but it gives

high costs and no flat region in the curve. In the region of 0.90 regenerator effectiveness, the costs given by this curve are about the same as those given by curves I and II. However, more regenerators are needed at 0.90 effectiveness than at 0.75 or 0.80; consequently, a more complex and costly ducting system results. The cost of the ducting was not included in Fig. 22.

The next step in the study was to investigate the relation between the allowable pressure losses and the size and cost of the ducting. To do this, it was necessary to adopt a typical gas system configuration and use the duct lengths, gas flow rates, densities, etc., of that system. Since the plant layout studies were carried out concurrently with but phased somewhat behind the analytical work, it was possible to converge closely on all the major dimensions required. (The system used was essentially that presented in Fig. 23.)

The results of detailed calculations of the pressure drop for the various elements of the ducting are presented in Table 3. It is instructive to note that the total length of ducting required by the reference design is about 2200 ft. Type 316 stainless steel was considered for the hot ducts at 1350°F, 1% Cr—0.5% Mo alloy steel for ducts in the temperature range 700°F to 1100°F, and A-212 grade B steel for ducts operating at temperatures less than 700°F. The results of detailed cost calculations for the duct system are presented in Table 4.

By examining Tables 3 and 4 together with Fig. 22, it can be deduced that the duct system giving minimum overall costs is one in which the ducts give a pumping power loss equivalent to about 2% of the reactor heat output. This follows from the fact that the pumping power losses vary inversely as the fifth power of the duct diameter, whereas the duct costs vary directly as the square of the diameter. Thus increasing the duct diameter 10% over that used in Tables 3 and 4 would increase the ducting cost about 20%, or about 0.02 mill/kwhr. At the same time, the pumping power losses chargeable to the ducts would be cut about 40%, and Fig. 22 indicates that this would save about 0.02 mill/kwhr. Thus the saving in costs associated with the reduction in duct pumping power losses would be roughly offset by the increased capital charges associated with the larger ducts. On the other hand, reducing the duct diameter would reduce the

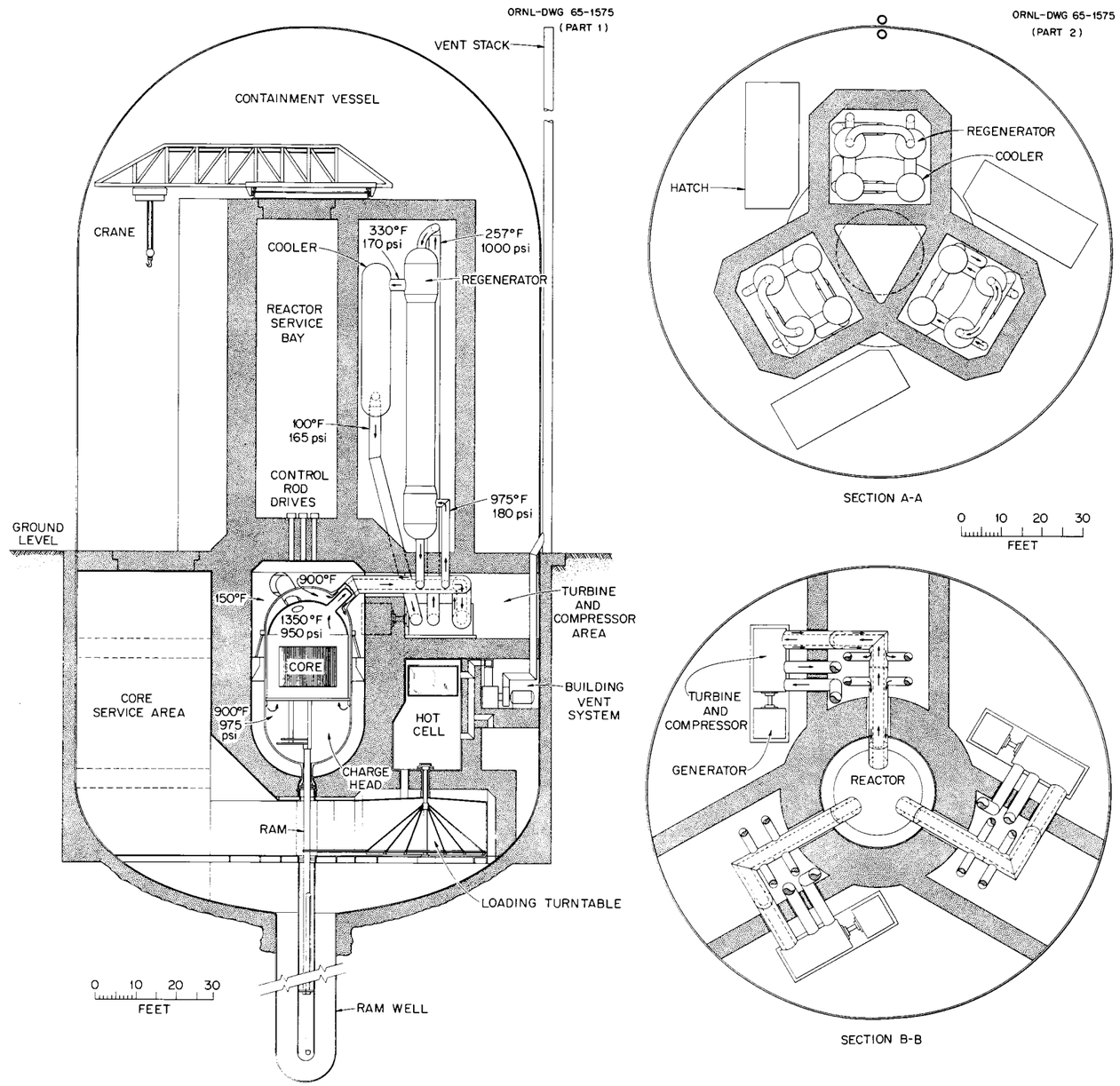

Fig. 23. Proposed 500-Mw(e) Direct-Cycle Power Plant.

Table 3. Duct Size and Pressure Drop for the Reference Power Plant

Total CO_2 flow rate in the cycle: 37.5×10^6 lb/hr
Regenerator effectiveness: 0.80
Ratio of pumping power for cycle to heat removal from reactor: 0.05

Location of Duct	1 Mean Temperature (°F)	2 P, Mean Pressure (psia)	3 L, Length for Each Duct (ft)	4 Number of Ducts	5 Total Duct Length (ft)	6 Duct Diameter (ft)	7 Total Duct Cross-Sectional Area (ft^2)	8 ρV (lb/ft·hr)[a]	9 ρ, Density (lb/ft^3)	10 ΔP_e, Exit and Entrance Losses[b] (psia)	11 ΔP_f, Friction Pressure Drop[c] (psia)	12 $\Delta P \equiv \Delta P_e + \Delta P_f$ (psia)	13 $(W/Q)^d$
								$\times 10^6$					$\times 10^{-2}$
Reactor to turbine	1350	950	60	3	180	3.5	28.9	1.30	2.15	6.58	0.65	7.23	0.41
Turbine to regenerator	975	180	45	6	270	4.5	95.5	0.393	0.513	2.51	0.16	2.67	0.63
Regenerator to cooler	330	170	15	6	90	4.0	75.5	0.496	0.898	2.29	0.04	2.33	0.32
Cooler to low-pressure compressor	100	165	80	6	480	3.5	57.8	0.652	1.210	2.93	0.36	3.29	0.33
Low-pressure compressor to intercooler	220	370	15	3	45	3.5	28.9	1.30	2.23	6.32	0.14	6.46	0.35
Intercooler to high-pressure compressor	100	365	15	3	45	3.5	28.9	1.30	2.69	5.25	0.11	5.36	0.25
High-pressure compressor to regenerator	257	1000	110	6	660	2.5	29.4	1.28	5.70	2.40	0.64	3.04	0.07
Regenerator to reactor	900	975	70	6	420	3.0	42.4	0.88	2.91	2.22	0.81	3.03	0.12
Total					2190								2.48

[a] $\rho V = \dfrac{(\text{total } CO_2 \text{ flow rate})}{(\text{total duct cross-sectional area})} = \dfrac{37.5 \times 10^6}{\text{column 7}}$.

[b] $\Delta P_e = \dfrac{\rho V^2}{2g \times 144}$.

[c] $\Delta P_f = 0.184 \ (Re)^{-0.2} \left(\dfrac{\rho V^2}{2g \times 144}\right) \times L$.

[d] $\dfrac{W}{Q} = \dfrac{(\text{pumping power})}{(\text{total heat removal from reactor})} = \dfrac{\Delta P}{778\rho} \dfrac{1}{c_p \ \delta t_{reactor}} =$

$\dfrac{1544T \ \Delta P}{778 \times 44P} \dfrac{1}{0.288 \times 520} = \dfrac{T}{3350} \dfrac{\Delta P}{P}$, where T is in °R .

Table 4. Cost of Ducts and Bellows for the Reference Plant

Location of Duct	Mean Temperature (°F)	Pressure (psia)	Length for Each Duct (ft)	Number of Ducts	Total Length of Duct (ft)	Duct Diameter (ft)	Number of Expansion Bellows	Unit Cost for Duct ($/ft)	Unit Cost for Bellows ($/bellows)	Duct Cost ($)	Bellows Cost ($)
										$\times 10^6$	$\times 10^6$
Reactor to turbine	1350	950	60	3	180	3.5	6	1600	25,000	0.298	0.150
Turbine to regenerator	975	180	45	6	270	4.5	12	850	15,000	0.239	0.180
Regenerator to cooler	330	170	15	6	90	4.0	6	600	8,000	0.048	0.048
Cooler to low-pressure compressor	100	165	80	6	480	3.5	12	450	6,000	0.216	0.072
Low pressure compressor to intercooler	220	370	15	3	45	3.5	3	450	6,000	0.020	0.018
Intercooler to high-pressure compressor	100	365	15	3	45	3.5	3	450	6,000	0.020	0.018
High-pressure compressor to regenerator	257	1000	110	6	660	2.5	12	450	5,000	0.297	0.060
Regenerator to reactor	900	975	70	6	420	3.0	18	850	19,000	0.357	0.342
Total					2190					1.505	0.888

Total cost of ducts and bellows = 2.393×10^6, $

$$= \frac{(2.39 \times 10^6) \times 1000 \times 0.14}{500,000 \times 6000}, \text{ mills/kwhr}$$

= 0.110 mills/kwhr net electrical output

duct capital charges about 0.02 mill/kwhr but would increase the duct pumping power-to-heat removal ratio to about 0.04 and increase the costs associated with the rest of the system by about 0.08 mill/kwhr. From this, it can be deduced that nearly minimum overall costs would be given by a set of duct diameters between that used in Tables 3 and 4 and a set about 10% larger; that is a set of duct diameters giving a pumping power-to-heat removal ratio between about 0.01 and 0.02 for the ducting.

Effects of Turbine Inlet Temperature on Costs

High turbine inlet temperatures improve the cycle efficiency and reduce the fuel cycle and capital costs. Figure 24 shows the effects of

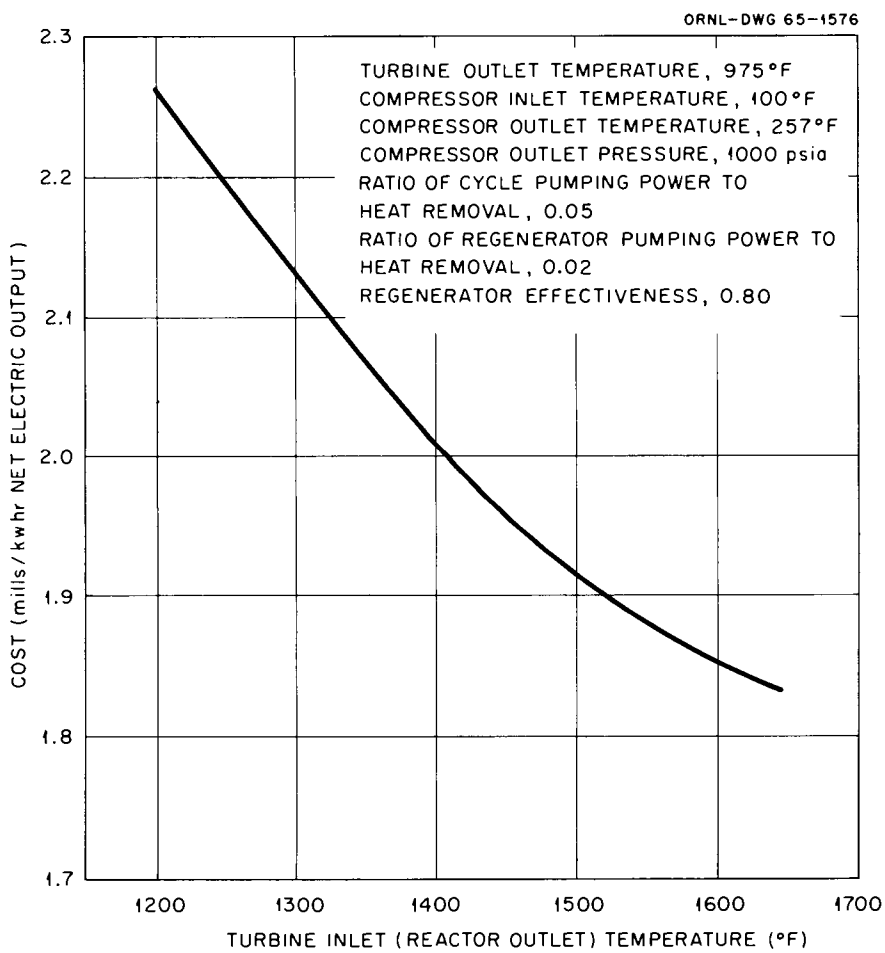

Fig. 24. Effects of Turbine Inlet Temperature on the Sum of Reactor Capital Charges and Fuel-Cycle, Regenerator, and Cooler Costs.

turbine inlet temperatures from 1200 to 1650°F on the sum of the reactor capital charges and the fuel-cycle, cooler, and regenerator costs. A regenerator effectiveness of 0.80 and pumping power-to-heat removal ratios of 0.05 for the cycle and 0.02 for the regenerator were used in this comparison. Other conditions were the same as those used for the bulk of the rest of the study and for the reference design of Fig. 23. Results of detailed calculations for the data shown in Fig. 24 are presented in Table 5.

The data in Fig. 24 indicate that, by increasing the turbine inlet temperature from 1200 to 1650°F, the reduction in the cost of the above components is equivalent to a saving of about 0.4 mill/kwhr in the power cost if no allowances are made for the higher costs of the more refractory materials that would be required. The higher temperature plants would have to employ many tons of high-alloy material, and this would increase charges substantially, though the amount is difficult to evaluate quantitatively. The adverse effect of high temperature on the cost of the turbine alone conceivably might more than offset the savings in the other costs.

Computer Codes

Upon completion of the preliminary studies carried out by hand calculations, a computer code was prepared for calculating the cycle efficiency and the power generation cost.[6] The basic analysis described previously was used in this code, except that the specific heat of CO_2, as obtained from ref. 13, was included in the program as a function of temperature and pressure. For a given set of temperature and pressure conditions, the computer was coded to the compressor split for intercooling that would yield the minimum compressor work, and then it calculated the cycle efficiency, the component cost, and the power generation cost directly chargeable to the reactor and gas-turbine system. Calculations repeated on the computer for the CO_2 cycle indicated that, when the compression process takes place near the saturation zone, the cycle efficiencies are 2 to 3% less than those obtained by hand calculations in

Table 5. Effect of Turbine Inlet Temperature on the Cost of the Reference Plant

Ratio of pumping power to heat removal: 0.05 for the cycle
0.02 for the regenerator

Regenerator effectiveness: 0.80

1	Turbine inlet temperature, °F	1200	1350	1500	1650
2	Turbine outlet temperature, °F	975	975	975	975
3	Compressor inlet temperature, °F	100	100	100	100
4	Compressor outlet temperature, °F	257	257	257	257
5	Gas temperature rise in reactor, δt_r, °F	465.5	518.5	572.5	631.5
6	Gas temperature rise in regenerator, δt_{reg}, °F	477	574	670	761
7	Gas temperature drop in cooler, δt_{cooler}, °F	278	301	325	349
8	Basic cycle efficiency (from Fig. 7)	0.306	0.332	0.354	0.371
9	Net cycle efficiency, E = basic cycle efficiency − 0.025	0.281	0.307	0.329	0.346
	Reactor				
10	Reactor capital and fuel-cycle costs (from Figs. 13 and 14), mills/kwhr	1.870	1.745	0.658	1.592
11	Reactor fuel-cycle cost (from Figs. 15 and 16), mills/kwhr	1.265	1.172	1.105	1.055
12	Reactor capital cost = /10/ − /11/, mill/kwhr	0.605	0.573	0.553	0.537
13	Reactor pressure vessel diameter (from Fig. 17), ft	17.6	17.0	16.5	16.3
14	Total CO_2 flow in the cycle = $(500{,}000 \times 3413)/(Ec_p\ \delta t_r)$, lb/hr	45.2×10^6	37.5×10^6	31.5×10^6	28.0×10^6
	Regenerators				
15	Length of regenerator tube (from Fig. 12), ft	60	60	60	60
16	Total cost of regenerators = (cost for reference plant) × (CO_2 flow rate in cycle)/(CO_2 flow rate in reference cycle), mills/kwhr	0.287	0.238	0.200	0.178
	Coolers				
17	Length of cooler tube, ft	24	24	24	24
18	Total cost of coolers = (cost for reference plant) × (CO_2 flow rate in cycle)/(CO_2 flow rate in reference cycle), mills/kwhr	0.105	0.087	0.073	0.065
19	Reactor and heat exchanger costs, /10/ + /16/ + /18/, mills/kwhr	2.262	2.070	1.911	1.835

which CO_2 is treated as a perfect gas (because the actual gas specific volume is somewhat greater than for a perfect gas).

Figure 25 shows the sum of the capital charges for the regenerator, cooler, and reactor and the reactor fuel-cycle costs as a function of

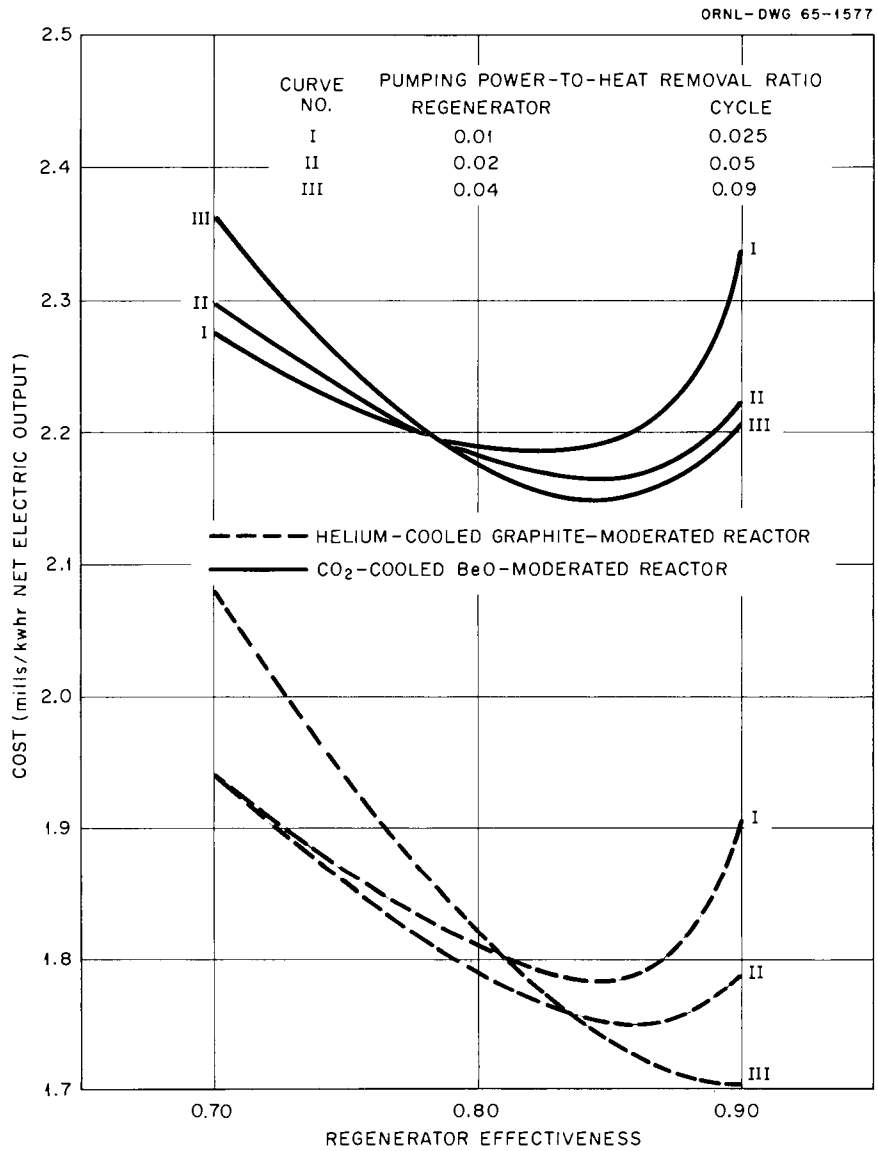

Fig. 25. Sum of Reactor Capital Charges and Fuel-Cycle, Regenerator, and Cooler Costs as a Function of Regenerator Effectiveness Based on Computer Calculations. Inclusion of compressor and turbine costs would bring the two sets of curves close together.

regenerator effectiveness for 1000-psia CO_2 and helium cycles as calculated by the computer. Temperatures of 1350°F at the turbine inlet, 975°F at the turbine outlet, and 100°F at the compressor inlet were selected for all cases. A BeO-moderated reactor was assumed for the CO_2 cycle and a graphite-moderated reactor for the helium cycle. The costs given by the computer calculation for the CO_2 cycle are about 0.15 mill/kwhr higher than the corresponding values shown in Fig. 21 for the same temperature and pressure conditions. The reason for this was the lower cycle efficiency obtained with the computer calculations because the compression process takes place near the saturation zone. A comparison of the costs for the CO_2 and helium cycles shown in Fig. 25 indicates that the cost for the helium cycle is about 0.35 mill/kwhr lower than that for the CO_2 cycle. This difference stems from the somewhat lower cost of the graphite-moderated reactor as compared with the BeO-moderated reactor and the higher shell-side heat transfer coefficients for the regenerator and cooler in the helium cycle. The latter effect results from the fact that the shell-side pressure was about 180 psia for the CO_2 system. The pressures in the ducts joining the turbines to the regenerators, the regenerators to the coolers, and the coolers to the compressors were also higher for the helium cycle and thus reduced the duct sizes.

Figure 26 shows the effect of compressor inlet temperature on the sum of the capital charges for the heat exchangers and the reactor and the reactor fuel-cycle costs for both helium and CO_2 systems.

The costs shown in Figs. 25 and 26 do not include the costs of the turbine and compressor units. The helium turbine and compressor would be larger in diameter and require about six times as many stages as the corresponding CO_2 units; hence the cost would run much higher — probably by at least $20/kw of net output. This would increase the capital charges for the helium system by about 0.5 mill/kwhr relative to the CO_2 system, and thus the 0.4 mill/kwhr advantage of the helium system indicated by Figs. 25 and 26 is deceptive — it would probably be more than offset by the higher costs of the helium turbine and compressor.

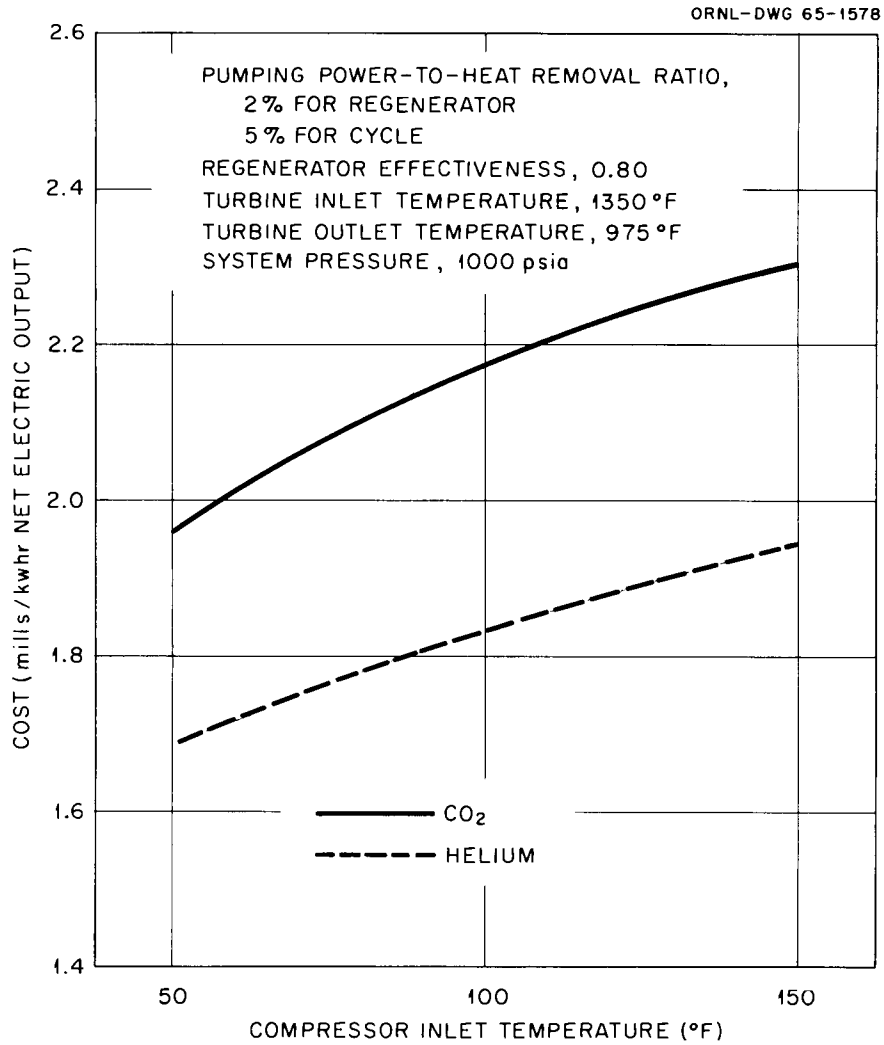

Fig. 26. Effect of Compressor Inlet Temperature on the Sum of Reactor Capital Charges and Fuel-Cycle, Regenerator, and Cooler Costs. Inclusion of compressor and turbine costs would bring the two curves close together.

Plant Layout

General Requirements

The first condition that it seemed desirable to impose in setting up criteria for the plant layout was that thermal convection should remove at least 3% of the full-power heat output of the reactor so that stoppage of all three turbine-generator units would not lead to serious overheating of the reactor and fuel elements. It was found that this

requirement could be met by any of several configurations if care were exercised in locating the components.

The second requirement that it seemed desirable to meet was that the pressure envelope should have no bellows expansion joints in the hot, high-pressure region, and, if possible, all bellows expansion joints should be eliminated from the gas system pressure envelope. No layout could be devised to meet the latter requirement, although the former could be met with a reasonable duct installation. While it was possible to eliminate bellows from a gas-turbine power plant designed for marine applications, the power output of that unit was intended to be only about 3% of the value chosen for this study. The low power of that system led to ducts sufficiently small in diameter and, hence, sufficiently flexible to permit the accommodation of thermal expansion without unduly complicating the system.

It was deemed essential that access to the turbine and compressor be provided to permit maintenance and replacement. To this end the shielding would be arranged so that there would be at least two 90-deg bends in any duct through the shield from the reactor to the turbine and at least one 90-deg bend in any shield duct from a heat exchanger. Further, the shielding around the turbine-compressor unit would be provided with a hatch so that the turbine-compressor unit could be removed with an overhead crane, placed in a large coffin on a railroad car, covered, and dispatched for major overhaul or repair work. Access to the heat exchangers was not considered necessary, but it was decided that the cooling-water lines to the cooler and intercooler should be manifolded outside the shield.

The containment vessel is a major cost item in the overall power plant, and hence the layouts were developed with a view toward minimizing the size and cost of this containment vessel consistent with meeting reasonable requirements for erection and maintenance of the plant. Hazards considerations made it necessary to place the turbine-generator units inside the containment shell. To minimize the cost of the concrete shielding, an effort was made to evolve a layout that would entail a minimum volume of concrete. To ease construction problems, a minimum clearance

of 3 ft was provided between the concrete and all components except ducts and core access tubes that pass through the shield.

Previous studies indicated that, for all-ceramic reactors, the fuel-handling operations should be carried out from the bottom of a reactor having its axis vertical.[1] The bulk of the layouts considered followed this approach.

Configuration Studies

Six layouts typical of those evolved for the overall system configuration are indicated in Fig. 27. It is evident from these that the need

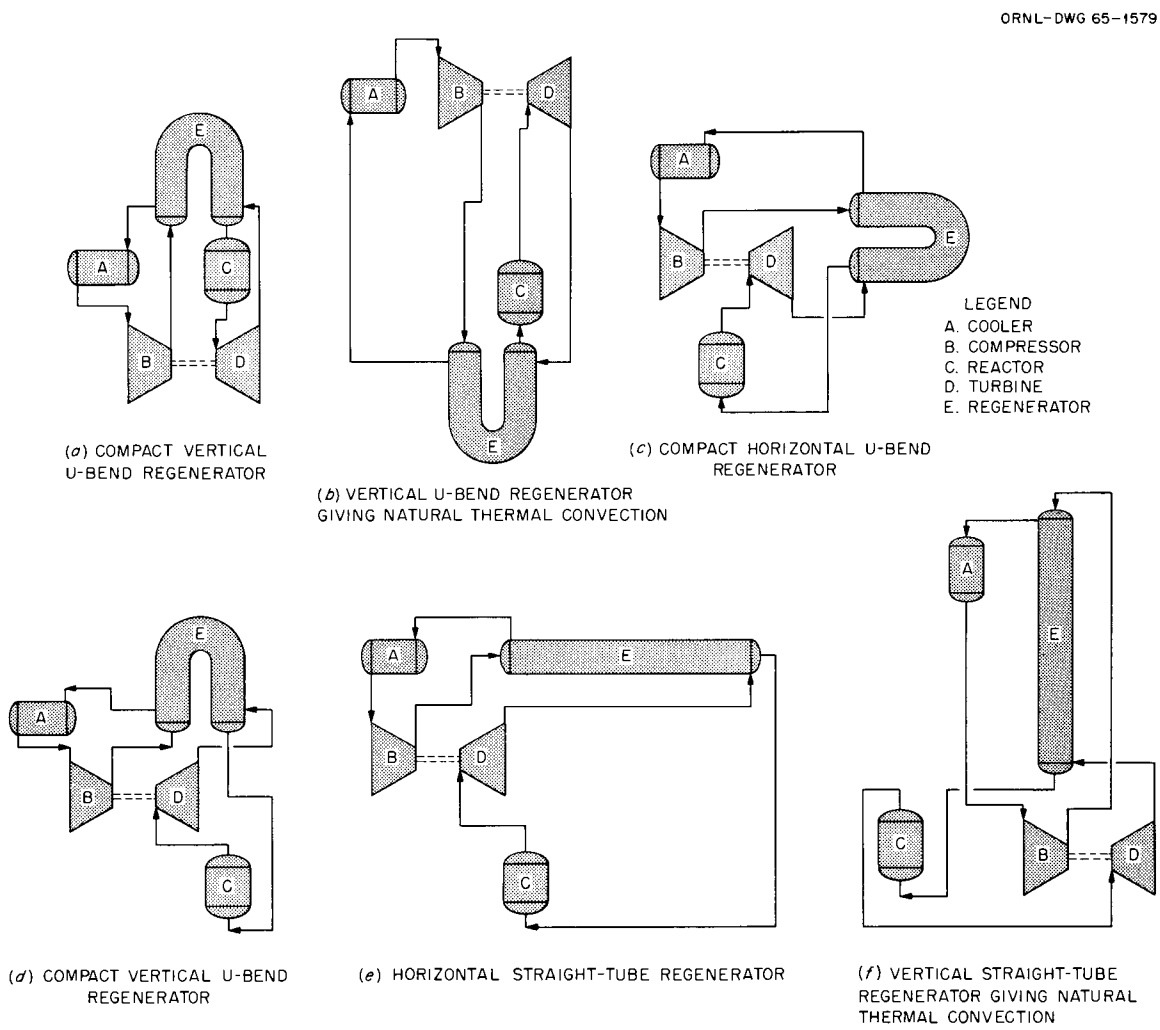

Fig. 27. Configurations for Gas-Turbine Power Plants.

to duct the gas back and forth between the turbine-compressor unit and the reactor and heat exchangers makes a complex ducting arrangement unavoidable. It can also be deduced from these layouts that conditions favorable to thermal convection are given only by configurations b and f, unless very long ducts are employed. In particular, the horizontal configurations of c and e are completely unsatisfactory in this respect, although they do have the advantage that the horizontal component of differential thermal expansion can be accommodated by mounting portions of the system on rollers. The configuration of Fig. 27f was chosen, since it showed the greatest promise of meeting the requirements outlined above.

Reference Design (HGCR-6)

A scale layout of the configuration shown schematically in Fig. 27f is presented in Fig. 23. Dimensional data for the reactor are given in Table 6. Three identical gas circuits are employed, each with its own

Table 6. Basic Data on the 500-Mw(e), BeO-Moderated Reactor Chosen for the HGCR-6

Coolant gas	CO_2
Core diameter, ft	13
Core height, ft	10
Reflector thickness, ft	1.4
Pressure vessel diameter, ft	17
Ratio of atoms of Be to atoms of ^{233}U	2000
Specific power, kw/kg of uranium	4000
Average core power density, kw/liter	27
Core void fraction	0.25
Fuel element[a] cross-sectional area, in.^{2}	0.22
Channel gross cross-sectional area, in.^{2}	1.13
Channel net gross cross-sectional area, in.^{2}	0.91
Hexagonal moderator block cross-sectional area, in.^{2}	3.65
Hexagonal moderator block distance across flats, in.	2.05

[a]Tubular fuel elements in circular channels through hexagonal moderator blocks.

turbine-compressor unit and related regenerators, coolers, and intercoolers. The pressures and temperatures in various elements of the system are indicated in Fig. 23. This configuration is favorable from the standpoint of thermal convection cooling; the system pressure envelope includes no expansion joints subject to both the full system pressure and the full system temperature, and the turbine-compressor units are not only adequately isolated by shielding from both the reactor and the heat exchangers but also are accessible for removal by the overhead crane.

One disadvantage of the layout shown is that it will require a large amount of ducting and many bellows expansion joints in the pressure envelope. There seems to be no way to avoid this if all the other requirements are to be met.

The requirement that the turbine-compressor unit be removable for maintenance poses some very difficult problems. The first approach considered was one in which the ducts leading to the unit would be cut and the unit as a whole removed. This has the disadvantage that rewelding the ducts and inspecting and leak-testing during the reinstallation would pose a host of difficult problems. In an effort to keep the turbine and compressor casings as leaktight as possible, the barrel-type construction employed for boiler feedwater pumps was considered with the thought that the casing could be left in place and the internals removed through a circular flanged joint at one end. This approach has the disadvantage that insertion of a long massive rotor and stator assembly axially in a horizontal position would be difficult. While the entire unit could be tipped up on end for vertical installation, this would have meant cutting all the ducts before the rotor and its stator assembly could be removed.

The possibility of splitting the casings on the horizontal centerline in the conventional fashion and bringing all the ducts into the lower half was examined. This would facilitate removal of the upper half of the casing and the turbine rotor and stator assemblies, and the lower half of the casing, a massive part, would be left welded into the system. A small seal weld or a brazed joint around the split in the casing would be necessary to give a satisfactory degree of fission-product retention. Unfortunately, cracking of this brazed or welded joint would be likely to prove

a problem, and the temperatures would be excessive for elastomer gaskets. A variation of this arrangement was finally chosen for the layout of Fig. 23, but it should be emphasized that this choice was simply for the purposes of the preliminary layout. The turbine-compressor unit was enclosed in a large tank with a thin welded cover. The split turbine casing was designed to carry the pressure loads but would not be expected to have a high degree of leaktightness. Fission products leaking through the horizontally split casing would be prevented from entering the surrounding room by the sealed outer tank. With this arrangement all close-clearance parts likely to give trouble would be incorporated in the turbine rotor and stator assemblies, which would be made so that they could be removed as units, complete with the bearings. The heavy casing would serve only as a pressure vessel and would have a minimum number of close clearances. The closure for the top cover of the relatively thin-walled outer tank would be readily accessible for seal welding, inspection, and leak testing, and distortion in this closure from the welding operation would have no effect on rotor or bearing alignment or clearances.

On removal of a rotor or a stator assembly, the unit would have to be raised, moved over, and lowered into a decontaminating tank and thoroughly cleaned. It could then be placed on a railroad car (brought through an air lock into the containment vessel) and shipped to the turbine manufacturer. It might be feasible to carry out decontamination operations before opening the turbine casing, but keeping water out of the rest of the system would be a problem.

Comparison of Steam- and Gas-Turbine Plants

The HGCR-4 steam plant of ref. 1, which served as the point of departure for this gas turbine study, and the HGCR-6 design of the previous section lend themselves nicely to a comparison of steam- and gas-turbine plants. The plants are similar except where the special requirements or problems of the gas-turbine plant made differences necessary.

Costs

Estimates of the absolute costs of nuclear plants are always both difficult to make and controversial, particularly for first-generation plants where design and development costs are such large factors and are often so hard to separate from fabrication, erection, and shakedown costs. Because of this, it seemed best for purposes of this comparison to consider only the basic costs for materials and fabrication of those items that differed between the two plants with no allowances for design, development, overhead, or contingency. On this basis, and assuming second- or third-generation plants, the estimates for the quantities of material required and the costs of comparable items for the steam- and gas-turbine plants are presented in Table 7.

The data of Table 7 indicate that the steam plant requires a smaller and less expensive heat exchanger, a smaller shield, much less in the way of duct work and thermal insulation, and a substantially smaller containment vessel. Further, the steam plant requires no bellows expansion joints in the gas ducts and a much less complex shield. While the steam plant requires an additional turbine building, the overall costs for essentially corresponding plants should be substantially lower for the steam system.

Although no attempt was made to include allowances for development costs in preparing Table 7, it should be remembered that the steam-turbine installation is made up of standard equipment that has been built, and large-capacity units are in operation. The gas turbines, on the other hand, are about ten times larger than any currently in operation, and hence, aside from development charges, there is a large uncertainty in the turbine costs for the gas-turbine plant, whereas there is not for the steam-turbine plant.

Maintenance

In comparing the steam- and gas-turbine plants from the standpoint of maintenance, it is clear that it would be far more difficult to repair or replace a gas-turbine and compressor unit than it would be to carry out a similar operation for a gas-circulating blower for a steam

Table 7. Comparative Costs of Major Items Directly Related to the Nuclear Portions of 500-Mw Net Electrical Output Gas-Turbine and Steam-Turbine Gas-Cooled Reactor Plants

Reactor: BeO-moderated, CO_2-cooled, 1000-psia system; reactor gas outlet temperature, 1350°F; specific power, 4000 kw/kg of U; moderator-to-uranium ratio, 2000; void fraction, 0.25

Gas-turbine cycle: Net cycle efficiency, 0.307; regenerator effectiveness, 0.80; total cycle pumping power-to-heat removal ratio, 0.05; turbine outlet temperature, 975°F; compressor inlet temperature, 100°F

Steam-turbine cycle: Net cycle efficiency, 0.425; superheated steam pressure, 2500 psia; temperature, 1050°F

	Gas-Turbine Plant			Steam-Turbine Plant		
	Dimensions or Quantity	Cost ($1000)	Capital Cost (mills/kwhr net output)[a]	Dimensions or Quantity	Cost ($1000)	Capital Cost (mills/kwhr net output)
Reactor building						
Concrete	24,000 yd^3	1,620		16,000 yd^3	1,080	
Containment shell and related items	150 ft diam 250 ft high	2,900		114 ft diam 179 ft high	1,600	
Building services and miscellaneous		1,850			1,420	
Total		6,370	0.297		4,100	0.191
Reactor						
Pressure vessel	710,000 lb 20 ft diam	2,030		430,000 lb 18 ft diam	860	
BeO in the core and reflector	450,000 lb	9,420		350,000	7,400	
Control rods and drives		440			440	
Miscellaneous insulation, etc.		300			260	
Installation		220			200	
Total		12,840	0.600		10,140	0.472
Turbine-generator units and auxiliaries		25,000	1.165		15,000	0.700
Turbine building					4,000	

[a]Plant capital cost was converted to mills/kwhr as follows:

$$\frac{(\text{plant capital cost, \$})(1000 \text{ mills/\$})(0.14 \text{ \$/\$-year})}{[(500{,}000 \text{ kw(e)}]\ (6000 \text{ hr/year})} = 0.0467 \times 10^{-6} \text{ mill/kwhr.}$$

Table 7. (continued)

	Gas-Turbine Plant			Steam-Turbine Plant		
	Dimensions or Quantity	Cost ($1000)	Capital Cost (mills/kwhr net output)[a]	Dimensions or Quantity	Cost ($1000)	Capital Cost (mills/kwhr net output)
Heat transfer equipment, blowers, and ducts						
Regenerator						
Tubing	1.030×10^6 lb	2,840				
Shells and headers	1.120×16^6 lb	2,250				
Coolers						
Tubing	0.413×10^6 lb	1,550			2,000	
Shells and headers	0.307×10^6 lb	300				
Steam generators				0.760×10^6 lb	3,200	
Installation and shipment		400			400	
Blowers					3,100	
Ducts, pipes, and manifolds		2,400			400	
Total		9,740	0.453		7,100	0.332
Coolant Charging and Storage						
Stack and vent gas system					100	
Pumps and tanks					500	
Total		1,200	0.056		600	0.028
Coolant purification		650	0.030		500	0.023
Fuel-handling and servicing equipment		3,000	0.139		2,500	0.117
Instrumentation and control		1,000	0.047		1,000	0.047
Sum of costs for basic plant components		59,800	2.787		40,940	1.910
Fuel-cycle cost			1.033[b]			0.798[b]
Sum of the costs for basic components and fuel-cycle costs		59,800	3.820		40,940	2.708

[b] In the fuel-cycle cost calculations, the charges for the fuel-handling equipment were included in the fuel-cycle cost. In this table, the fuel-handling equipment was introduced as a plant capital charge. Therefore, the power cost equivalent to the fuel-handling equipment was deducted from the fuel-cycle cost.

plant. The gas turbine gives at least a factor of 10 increase in the size and surface area subject to fission-product deposition, and it will present the first surface substantially cooler than the core to be encountered by the gas leaving the reactor. As a result, the activity deposited in the turbine per unit of area would probably be much greater than in the gas-circulating blower of a steam plant. Perhaps even more important is the fact that the blower for the steam plant could be installed with a flange in a cool zone so that an elastomer gasket could be employed in the unit itself. Such an installation seems out of the question for a gas-turbine plant; welded joints would have to be cut or an additional external tank with cooling provisions would have to be installed around the turbine and coupled to the buffer-gas system.

Hazards

In comparing the gas-turbine and steam-turbine plants from the reactor safeguards standpoint, it is evident that the contaminated-gas-system pressure envelope for the steam-turbine plant is simpler, more rugged, and much less likely to leak. Further, differential thermal expansion can be accommodated without introducing bellows into the pressure envelope, and the volume of contained gas per kilowatt of capacity is smaller. On the other hand, the possibility of hydrogen formation from the water-gas reaction would be completely avoided in the gas-turbine plant if a graphite moderator were employed.

Thermal Efficiency

It is interesting to compare the thermal efficiency of the gas- and steam-turbine plants using the results of this study. Figure 7 shows the gas-turbine plant efficiency as a function of turbine inlet temperature. Curves in Fig. 22 for minimum overall costs indicate that the lowest costs are given by a regenerator effectiveness of about 0.80 and a pumping power-to-heat removal ratio of about 0.025. Extrapolation of the curve for these conditions in Fig. 7 indicates that a turbine inlet temperature of about 2000°F would be required to give a plant efficiency of 42.7%, which is the efficiency of the corresponding steam-turbine plant operating with

a 1350°F gas temperature and a 1050°F steam temperature, as presented in ref. 1.

Application of More Complex Gas-Turbine Systems

A relatively simple gas-turbine system was employed to provide a clear-cut basis for comparison with the reference steam-turbine plant. Among the variations considered for further studies were (1) driving the compressor at a more economical speed by a separate gas turbine, (2) reducing the size of the containment vessel by various means, such as placing the electric generator in a blister or providing more compact means for disassembly and handling of components, and (3) using the gas turbine as a topping unit superimposed on a steam-generator and steam-turbine plant. However, the study covered in this report indicates that the maintenance and hazards problems — the truly crucial problems of all-ceramic high-temperature gas-cooled reactors — are much more difficult than in corresponding steam plants. Further, a host of thermodynamic cycle studies reported in the literature show that little improvement in cycle efficiency can be obtained by going to more complex cycles than that considered here. The writers believe that whatever improvements could be achieved would have little effect on the cost advantage of the steam-turbine plant, as indicated by Table 7. While it may be argued that the gas-turbine plant can employ higher gas temperatures to better advantage than a steam-turbine plant, it should be remembered that the fuel elements in the hot zone will run 300 to 500°F above the reactor gas outlet temperature, and increasing the fuel temperature would have an adverse effect on the fission-product release rate. In view of all these factors, it appears to the writers that there is little incentive for investigating further modifications and refinements of the gas-turbine system.

References

1. A. P. Fraas, Preliminary Designs for Four Integrated Gas-Cooled Reactor Core and Steam Generator Units, USAEC Report ORNL-2752, Oak Ridge National Laboratory, Nov. 23, 1962.

2. J. C. Bokros and H. E. Shoemaker, Reactor Materials Compatibility with Impurities in Helium, USAEC Report GA-1508, General Atomic Jan. 12, 1961.

3. A. S. Thompson, Studebaker-Packard Corp., to A. P. Fraas, Oak Ridge National Laboratory (personal communication).

4. General Atomic, Evaluation of Coolants and Moderators for the Maritime Gas-Cooled Reactor, USAEC Report GA-570, December 1958.

5. H. C. Carney, Jr., Conceptual Design Study of a 3000-Kwe Mobile Nuclear Power Plant, USAEC Report AGN TM-383, Aerojet-General Nucleonics, April 1961.

6. R. V. Miskell, Effects of Major Parameters on Cycle Efficiency and Cost of a Gas-Cooled Reactor Turbine Power Plant, Thesis in Nuclear Engineering, University of Tennessee, Report Y-1396, Union Carbide Nuclear Co., June 19, 1962.

7. J. H. Keenan and J. Kaye, Gas Tables, Wiley, New York, 1948.

8. A. P. Fraas and M. N. Ozisik, Steam Generators for High-Temperature Gas-Cooled Reactors, USAEC Report ORNL-3208, Oak Ridge National Laboratory, April 4, 1963.

9. ASME Pressure Vessel Code, American Society of Mechanical Engineers, New York, 1964.

10. The Babcock & Wilcox Co., Steam — Its Generation and Use, 37th ed., Geo. McKibbin & Son, New York, 1955.

11. Oak Ridge National Laboratory, The ORNL Gas-Cooled Reactor, Part 4, Plant Design, USAEC Report ORNL-2500, p. 11.3, Apr. 1, 1958.

12. A. P. Fraas and M. N. Ozisik, Relative Capital Charges and Fuel Cycle Costs for All-Ceramic Gas-Cooled Reactors, USAEC Report ORNL-CF 60-7-41, Oak Ridge National Laboratory, July 20, 1960.

13. J. Hilsenrath et al., Tables of Thermodynamic and Transport Properties of Air, Argon, Carbon Dioxide, Carbon Monoxide, Hydrogen, Nitrogen, Oxygen, and Steam, NBS Circular 564, Pergamon Press, 1960.

14. Max Jakob, Heat Transfer, Vol. II, p. 205, Wiley, New York, 1957.

15. J. G. Knudsen and D. L. Katz, Fluid Dynamics and Heat Transfer, pp. 420–421, McGraw-Hill, New York, 1958.

16. W. M. Kays and A. L. London, Compact Heat Exchangers, p. 9, McGraw-Hill, New York, 1958.

17. Max Jakob, Heat Transfer, Vol. II, pp. 207–208, Wiley, New York, 1957.

Nomenclature

A	Flow area, ft^2
A_1, A_2	Outside and inside flow areas per tube, respectively, ft^2
c_p	Specific heat of gas (fluid) at constant pressure, Btu/lb·°F
D_1, D_2	Outside and inside diameters of tube, ft
D_e	Equivalent diameter for flow, ft
E	Efficiency
F	$A_1/A_2 = G_2/G_1$ (Eqs. B.23 and B.26)
f	Friction factor, dimensionless
g	Acceleration due to gravity, ft/hr^2
G_1, G_2	Mass flow rates of gas per unit area of passage outside and inside the tube, $lb/ft^2 \cdot hr$
k	Thermal conductivity of gas (fluid), $Btu/hr \cdot ft^2$ (°F/ft)
h	Coefficient of heat transfer, $Btu/hr \cdot ft^2 \cdot °F$
h_1, h_2	Coefficients of heat transfer of gas (fluid) outside and inside the tube, $Btu/hr \cdot ft^2 \cdot °F$
H	Heat content of gas, Btu/lb
L	Length of tube, ft
M	Molecular weight of gas, lb/mole
M'	Total flow rate of gas in the regenerator or cooler, lb/hr
m_1, m_2	Mass flow rates of gas per tube outside and inside the tube, lb/hr·tube
N	Number of tubes per heat exchanger
n	Specific heat ratio
P	Pressure, psia
dP	Differential pressure in velocity heads for differential length dX
ΔP	Pressure difference in velocity heads for length L
$\overline{\Delta P}$	Pressure difference, psia
Pr	Prandtl number, dimensionless
Q	Heat transfer rate across a tube of the heat exchanger, Btu/hr·tube
q	Heat flow, Btu/hr
dS	Differential area along the tube for a differential length dX, ft^2

s_1, s_2	Heat transfer surface areas per tube (for entire length L), ft^2
S_1, S_2	Outside and inside total heat transfer areas per tube, respectively, ft^2
T	Temperature, °R
T_{1i}, T_{2i}	Inlet temperatures of hot and cold gas into the regenerator, °R
T_w	Tube wall temperature, °R
t	Temperature, °F
U	Overall coefficient of heat transfer, $Btu/ft^2 \cdot hr \cdot °F$
V	Velocity of gas, ft/hr
W	Pumping power per tube, Btu/hr·tube
x	Length along the tube, ft
dx	Differential length, ft
B	Factor defined in Fig. 12 and Appendix D
Z	Factor defined in Eq. A.5
α	Factor defined by Eq. B.20
λ	Parameter in heat and mass transfer analogy
ϵ_i, ϵ_o	Coefficients measuring inlet and outlet losses in velocity heads, dimensionless
ρ	Density of gas, lb/ft^3
τ_1	$\frac{T_{1o}}{T_{1i}} = 1 - \frac{\delta t}{T_{1i}} = 1 - \eta \left(1 - \frac{T_{2i}}{T_{1i}}\right)$ (Eq. B.16)
τ_2	$\frac{T_{2o}}{T_{2i}} = 1 + \frac{\delta t}{T_{2i}} = 1 + \eta \left(\frac{T_{1i}}{T_{2i}} - 1\right)$ (Eq. B.18)
δt	Temperature rise of gas in the regenerator, °F
θ	Temperature difference between the bulk gas (fluid) temperature and the tube wall temperature, °F
θ_{ln}	Logarithmic mean temperature difference, defined by Eq. C.6, °F
μ	Viscosity of gas, lb/ft·hr
η	$\delta t/(T_{1i} - T_{2i})$ = regenerator effectiveness
γ	(Outside diameter of tube)/(inside diameter of tube), dimensionless

Subscripts

1	Refers to hot gas or outside of tube
2	Refers to cold gas or inside of tube
i,o	Refer to inlet and outlet
1i,1o	Inlet and outlet for hot gas
2i,2o	Inlet and outlet for cold gas
1f,2f	Friction for hot and cold gases
LPC	Low-pressure compressor
HPC	High-pressure compressor
t	Turbine

APPENDICES

Appendix A

CYCLE EFFICIENCY

The basic thermal efficiency for the closed cycle shown in Figs. 3 and 4 is

$$E = \frac{(\text{turbine work}) - (\text{compressor work})}{(\text{heat supplied by the reactor})} , \tag{A.1}$$

where

turbine work = $(\Delta h)_{6-7}$,

compressor work = $(\Delta h)_{2-1} + (\Delta h)_{4-3}$,

heat supplied by the reactor = $(\Delta h)_{6-5}$,

$\Delta h = c_p \, \delta t$.

The subscripts refer to the actual gas condition at the location indicated in Fig. 3. The actual gas temperatures T_1, T_3, T_4, T_6, and T_7 were all fixed, and $T_5 = T_4 + \delta t_{regenerator}$. Therefore, for a given value of $\delta t_{regenerator}$, the only unknown quantity in Eq. (A.1) is T_2, which can be evaluated from Eq. (A.2).

Across the low-pressure compressor,

$$T_2 = T_1 \left\{ 1 + \frac{1}{E_{LPC}} \left[\left(\frac{P_2}{P_1} \right)^{(n-1)/n} - 1 \right] \right\} . \tag{A.2}$$

The unknown pressures P_1 and P_2 are

$$P_1 = P_4 - (\text{pressure drop across the turbine}) - (\text{friction drop over the cycle, excluding that across the intercooler}) \tag{A.3}$$

and

$$P_2 = \frac{P_4}{\left[1 + E_{HPC} \left(\frac{T_4}{T_3} - 1 \right) \right]^{(n-1)/n}} + (\text{friction pressure drop across the intercooler}) . \tag{A.4}$$

In these equations, P_4 is the pressure at the outlet of the high-pressure compressor, which is assumed to be known. The pressure drops can be calculated from Eq. (A.5).

The pressure drop across the turbine, $\overline{\Delta P}_{6-7}$, is

$$\overline{\Delta P}_{6-7} = P_6 - P_7 = P_6(1 - Z) \ , \tag{A.5}$$

where

$$Z = \left(\frac{P_6}{P_7}\right) = \left[1 - \frac{1}{E_t}\left(1 - \frac{T_7}{T_6}\right)\right]^{n\lambda n-1} .$$

The friction pressure drops depend on the flow rate and the flow passage dimensions. The cycle efficiencies can therefore be calculated if the allowable friction pressure drops along the cycle are known. It is also possible to relate the friction pressure drop to the pumping power-to-heat removal ratio, as follows:

$$\text{Pumping power} \equiv W = \frac{1}{778}\,\frac{GA}{\rho}\,\overline{\Delta P} \ , \tag{A.6}$$

in Btu/hr, and

$$\text{Heat removal} \equiv Q = G\ A\ c_p\ \delta t \ , \tag{A.7}$$

in Btu/hr. Assuming a perfect gas,

$$\rho = \frac{PM}{1544\ T} \ , \tag{A.8}$$

in lb/ft^3. From Eqs. (A.6), (A.7), and (A.8),

$$\frac{\overline{\Delta P}}{P} = 0.503\ \frac{M' c_p\ \delta t}{T}\left(\frac{W}{Q}\right) . \tag{A.9}$$

Appendix B

PUMPING POWER-TO-HEAT REMOVAL RATIO AND TUBE LENGTH FOR A COUNTERFLOW REGENERATOR

Pumping Power-to-Heat Removal Ratio

The temperature profiles for the hot and cold fluids of a counterflow regenerator in a closed cycle are two parallel straight lines,[14] as illustrated in Fig. B.1, assuming $m_1 c_{p1} = m_2 c_{p2}$. In this figure, fluid 1 refers to the hot fluid and fluid 2 refers to the cold fluid.

The total pressure drop is composed of inlet, friction, and outlet pressure drops. The inlet and outlet pressure drops can be expressed, in velocity heads, as follows:

$$\Delta P_{1i} = \epsilon_{1i} \frac{V_{1i}^2}{2g} , \tag{B.1}$$

$$\Delta P_{1o} = \epsilon_{1o} \frac{V_{1o}^2}{2g} . \tag{B.2}$$

The friction pressure drop, in velocity heads, for a differential section (dX) is

$$dP_{1f} = -4f \frac{V_1^2}{2g} \frac{dx}{D_{e1}} . \tag{B.3}$$

The total friction pressure drop, in velocity heads, for the length L is

$$\Delta P_{1f} = \int_0^L dP_1 = - \int_0^L \frac{2f}{D_{e1}} \frac{V_1^2}{g} dx . \tag{B.4}$$

From the heat-transfer and mass-transfer analogy*

$$\frac{2f}{D_{e1}} dx = \frac{1}{\lambda} \frac{dT_1}{T_1 - T_w} , \tag{B.5}$$

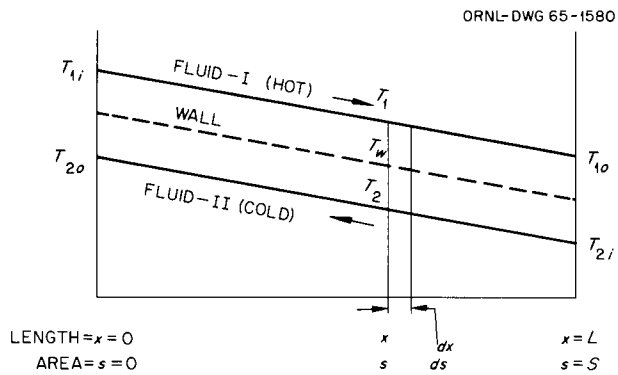

Fig. B.1. Temperature Profile for Regenerator.

where λ is the parameter commonly used in this relation. From Eqs. (B.4) and (B.5)

$$\Delta P_{1f} = - \int_{T_{1i}}^{T_{1o}} \frac{1}{\lambda} \frac{dT_1}{T_1 - T_w} . \tag{B.6}$$

The total pumping power for fluid-1 is

$$W_1 = \frac{A_1 G_1}{778} (\Delta P_{1f} + \Delta P_{1i} + \Delta P_{1o}) . \tag{B.7}$$

---

*$dq = h$ (perimeter) $dx\ (T_1 - T_w) = G\rho$ (cross-sectional area) dt_1 , or

$$\frac{h}{G\rho} = D_{el} \frac{dT_1}{T_1 - T_w} \frac{1}{4\ dx} .$$

On the basis of the mass-transfer analogy,

$$\frac{h}{G\rho} = \frac{f}{2} \lambda ,$$

and hence

$$\frac{2f}{D_{el}} dx = \frac{1}{\lambda} \frac{dT_1}{T_1 - T_w} ,$$

where

$\lambda = 1$ in Reynolds analogy,

$$= \frac{1}{1 + 5(f/2)^{1/2} (Pr - 1)} \text{ in Prandtl analog.}$$

Substituting Eqs. (B.1), (B.2), and (B.6) into Eq. (B.7) gives

$$W_1 = \frac{A_1 G_1}{778} \int_{T_{1o}}^{T_{1i}} \frac{1}{\lambda} \frac{V_1^2}{g} \frac{dT_1}{T_1 - T_w} + \epsilon_{1i} \frac{V_{1i}^2}{2g} + \epsilon_{1o} \frac{V_{1o}^2}{2g} . \tag{B.8}$$

Assuming a perfect gas, $\rho = \frac{PM}{1544T}$, and hence

$$V^2 = \frac{G^2}{\rho^2} = G^2 \frac{(1544)^2 T^2}{P^2 M^2} . \tag{B.9}$$

Substituting Eq. (B.9) into Eq. (B.8), assuming P, G, and $(T_1 - T_w)$ are constant, and integrating (i.e., P can be assumed constant for small pressure drops, and $T_1 - T_w$ is also constant, as shown in Fig. 28) gives

$$W_1 = \frac{A_1 G_1^3 (1544)^2}{(2 \times 778) g P_1^2 M^2} \left[\frac{2}{3} \frac{T_{1i}^3 - T_{1o}^3}{\lambda (T_1 - T_w)} + \left(\epsilon_{1i} T_{1i}^2 + \epsilon_{1o} T_{1o}^2 \right) \right] . \tag{B.10}$$

The heat transferred across the regenerator is

$$Q = A_1 G_1 c_p (T_{1i} - T_{1o}) . \tag{B.11}$$

Dividing Eq. (B.10) by Eq. (B.11) gives

$$\left(\frac{W_1}{Q} \right) = \frac{G_1^2 (1544)^2}{1556 g P_1^2 M^2 c_p} \left[\frac{2}{3} \frac{1}{\lambda (T_1 - T_w)} \frac{T_{1i}^3 - T_{1o}^3}{T_{1i} - T_{1o}} + \frac{\epsilon_{1i} T_{1i}^2 + \epsilon_{1o} T_{1o}^2}{T_{1i} - T_{1o}} \right] . \tag{B.12}$$

Assuming $H_1 \cong h_2$,

$$T_1 - T_w \cong \frac{T_{1o} - T_{2i}}{2} . \tag{B.13}$$

Let

$$\tau_1 = \frac{T_{1o}}{T_{1i}} \quad (<1) . \tag{B.14}$$

Substituting Eqs. (B.13) and (B.14) into Eq. (B.12) gives

$$\left(\frac{W_1}{Q}\right) = \frac{G_1^2(1544)^2 T_{1i}}{1556 g P_1^2 M^2 c_p} \left[\frac{4}{3} \frac{1 + \tau_1 + \tau_1^2}{\lambda \left(\tau_1 - \frac{T_{2i}}{T_{1i}}\right)} + \frac{\epsilon_{1i} + \tau_1^2 \epsilon_{1o}}{1 - \tau_1}\right] . \tag{B.15}$$

Sometimes it is desirable to introduce the regenerator effectiveness, η, instead of the above parameter, τ_1. Assuming $m_1 c_{p1} = m_2 c_{p2}$, the regenerator effectiveness is

$$\eta \equiv \frac{\delta t}{(T_{1i} - T_{2i})} ,$$

and the relation between τ_1 and η is

$$\tau_1 = \frac{T_{1o}}{T_{1i}} = 1 - \frac{\delta t}{T_{1i}} = 1 - \eta \left(1 - \frac{T_{2i}}{T_{1i}}\right) . \tag{B.16}$$

Following a similar procedure for the cold fluid,

$$\left(\frac{W_2}{Q}\right) = \frac{G_2^2(1544)^2 T_{2i}}{1556 g P_2^2 M^2 c_p} \left[\frac{4}{3} \frac{1 + \tau_2 + \tau_2^2}{\lambda \left(\frac{T_{1i} - \tau_2}{T_{2i}}\right)} + \frac{\epsilon_{2i} + \tau_2^2 \epsilon_{2o}}{\tau_2 - 1}\right] , \tag{B.17}$$

where

$$\tau_2 = \frac{T_{2o}}{T_{2i}} = 1 + \frac{\delta t}{T_{2i}} = 1 + \eta \left(\frac{T_{1i}}{T_{2i}} - 1\right) . \tag{B.18}$$

The total pumping power-to-heat removal ratio for the regenerator is the sum of Eqs.(B.15) and (B.17).

Tube Length

From ref. 17,

$$T_{1o} = \frac{\alpha T_{2i} + T_{1i}}{1 + \alpha} , \tag{B.19}$$

where

$$\alpha = \frac{US}{mc_p} \ . \tag{B.20}$$

Solving Eq. (B.19) for α and replacing (T_{1o}/T_{1i}) by $\left(1 - \frac{\delta t}{T_{1i}}\right)$, gives

$$\alpha = \frac{\delta t}{T_{1i} - T_{2i} - \delta t} \ . \tag{B.21}$$

Assuming that the wall resistance to heat flow is negligible compared with the fluid film resistances, the overall coefficient of heat transfer is

$$U = \frac{1}{\frac{1}{h_1} + \frac{1}{h_2}} \ . \tag{B.22}$$

For a closed cycle:

$$A_1 G_1 = A_2 G_2$$

or, let

$$\frac{G_2}{G_1} = \frac{A_1}{A_2} \equiv F \ . \tag{B.23}$$

If fluid 2 (i.e., the cold fluid) flows inside the tube, the equivalent hydraulic diameter for flow outside the tubes of an infinite array of tubes is

$$D_e = \frac{4A_1}{\pi D_1} \ ,$$

or

$$A_1 = \frac{\pi}{4} D_1 D_e = \frac{\pi}{4} \gamma \ D_2 D_e \ , \tag{B.24}$$

where

$$\gamma \equiv \frac{\text{(outside diameter)}}{\text{(inside diameter)}} = \frac{D_1}{D_2}$$

and

$$A_2 = \frac{\pi}{4} D_2^2 \ . \tag{B.25}$$

Substituting Eqs. (B.24) and (B.25) into Eq. (B.23) gives

$$F = \frac{A_1}{A_2} = \frac{\gamma D_e}{D_2} = \frac{G_2}{G_1} \ . \tag{B.26}$$

The heat transfer coefficients h_1 and h_2 for the fluids based on the internal tube surface are, for the inside fluid,

$$h_2 = 0.023\ k_2 \frac{Pr_2^{0.4}}{\mu_2^{0.8}} G_2^{0.8} D_2^{-0.2} \ , \tag{B.27}$$

and, for the outside fluid,

$$h_1 = \gamma \left(0.023\ k_1 \frac{Pr_1^{0.4}}{\mu_1^{0.8}} G_1^{0.8} D_e^{-0.2}\right) \ . \tag{B.28}$$

Assuming $k_1 = k_2$, $Pr_1 = Pr_2$, and $\mu_1 = \mu_2$, Eqs. (B.27) and (B.28) in conjunction with Eq. (B.26) gives

$$\frac{h_2}{h_1} = \frac{1}{\gamma}\left(\frac{G_2}{G_1}\right)^{0.8}\left(\frac{D_e}{D_2}\right)^{0.2} = \frac{1}{\gamma} F^{0.8}\left(\frac{F}{\gamma}\right)^{0.2} = \frac{F}{\gamma^{1.2}}$$

or

$$\frac{1}{h_1} = \frac{F}{\gamma^{1.2}} \frac{1}{h_2} \ . \tag{B.29}$$

Substituting Eq. (B.29) into Eq. (B.22), gives the overall coefficient of heat transfer based on the internal tube surface as

$$U = h_2 \left(1 + \frac{F}{\gamma^{1.2}}\right)^{-1} . \tag{B.30}$$

Taking

$$S = \pi D_2 L$$

$$M = \frac{\pi}{4} D_2^2 G_2 \tag{B.31}$$

and substituting Eqs. (B.30) and (B.31) into Eq. (B.20) gives

$$\alpha = 4 \left(1 + \frac{F}{\gamma^{1.2}}\right)^{-1} \frac{h_2 L}{D_2 G_2 c_p} . \tag{B.32}$$

Then, substituting Eq. (B.27) into Eq. (B.28) and rearranging the terms to suppress μ gives

$$\alpha = 0.092 \left(1 + \frac{F}{\gamma^{1.2}}\right)^{-1} \left(\frac{k_2^{0.2}}{c_{p2}^{0.2}\ Pr_2^{0.4}}\right) G_2^{-0.2}\ D_2^{-1.2}\ L . \tag{B.33}$$

Eliminating α between Eqs. (B.21) and (B.33) and solving for L,

$$L = 10.9 \left(1 + \frac{F}{\gamma^{1.2}}\right) \left(\frac{c_{p2}^{0.2}\ Pr^{0.4}}{k_2^{0.2}}\right) G_2^{0.2}\ D_2^{1.2}\ \frac{\delta t}{T_{1i} - T_{2i} - \delta t} . \tag{B.34}$$

Appendix C

PUMPING POWER-TO-HEAT REMOVAL RATIO AND TUBE LENGTH FOR A COUNTERFLOW COOLER WITH CONSTANT WALL TEMPERATURE

Pumping Power-to-Heat Removal Ratio

The temperature profile for the hot fluid in a counterflow cooler with a constant wall temperature can be represented as shown in Fig. C.1. Following the same procedure as in Appendix B, the total pumping power for the hot fluid is (from Eq. B.8, with $T = T_w = \theta$ and $dT = d\theta$)

$$W_1 = \frac{A_1 G_1}{778}\left(-\int_{\theta_i}^{\theta_o} \frac{1}{\lambda}\frac{V_2^2}{g}\frac{d\theta}{\theta} + \epsilon_i \frac{V_i^2}{2g} + \epsilon_o \frac{V_o^2}{2g}\right) \tag{C.1}$$

and

$$V^2 = \frac{G_1^2(1544)^2 T^2}{P_1^2 M^2} . \tag{C.2}$$

Substituting Eq. (C.1), assuming that variations in T and P are negligible so that they can be treated as constants, and performing the integration gives

$$W = \frac{A_1 G_1^3 (1544)^2 T^2}{1556 g P^2 M^2}\frac{2}{\lambda}\ln\frac{\theta_i}{\theta_o} + (\epsilon_i + \epsilon_o) . \tag{C.3}$$

The heat removal in the cooler is

$$Q = A_1 G_1 c_p(\theta_i - \theta_o) . \tag{C.4}$$

Dividing Eq. (C.3) by Eq. (C.4) gives

$$\left(\frac{W_1}{Q}\right) = \frac{G_1^2(1544)^2 T^2}{1556 g P_1^2 M^2 c_p(\theta_i - \theta_o)}\left[\frac{2}{\lambda}\ln\frac{\theta_i}{\theta_o} + (\epsilon_i + \epsilon_o)\right] . \tag{C.5}$$

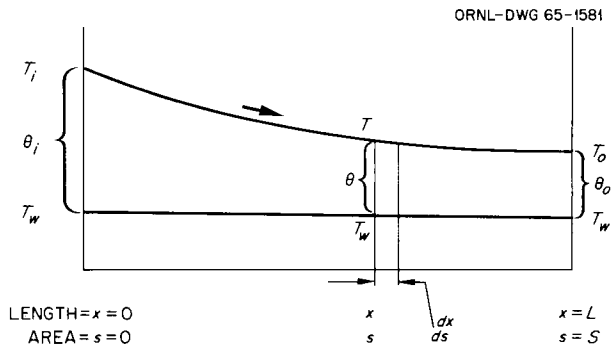

Fig. C.1. Temperature Profile for Cooler.

Let

$$\theta_{ln} = \frac{\theta_i - \theta_o}{\ln \frac{\theta_i}{\theta_o}} \tag{C.6}$$

and

$$T_w = \text{tube wall temperature, } ^\circ R \ .$$

Then,

$$T = T_w + \theta_{ln} \ . \tag{C.7}$$

Rearranging Eq. (C.5) gives

$$\left(\frac{W_1}{Q}\right) = \frac{G_1^2 (1544)^2 (T_w + \theta_{ln})^2}{1556 g P_1^2 M^2 c_p} \left(\frac{2}{\lambda} \frac{1}{\theta_{ln}} + \frac{\epsilon_i + \epsilon_o}{\theta_i - \theta_o}\right) . \tag{C.8}$$

<u>Tube Length</u>

The heat transfer relations for a differential section (ds) of the cooler are

$$h \ ds \ \theta = mc_p \ d\theta$$

or

$$-d\theta = \frac{\theta h}{mc_p}\, dS \ . \tag{C.9}$$

Integrating Eq. (C.9) from s = 0 to s = S gives

$$\ln \frac{\theta_i}{\theta_o} = \frac{hS}{mc_p} \ . \tag{C.10}$$

The hot gas (fluid 1) is assumed to flow outside the tube, and

$$F \equiv \frac{A_1}{A_2} = \frac{A_1}{\frac{\pi}{4} D_2^2} \ , \tag{C.11}$$

$$m_1 = A_1 G_1 \ , \tag{C.12}$$

$$s_1 = \pi D_1 L \ , \tag{C.13}$$

$$h_1 = 0.023\ k_1\ (D_e)^{-0.2}\ G_1^{0.8}\ \frac{Pr_1^{0.4}}{\mu_1^{0.8}} \ . \tag{C.14}$$

Substituting Eqs. (C.11), (C.12), (C.13), and (C.14) into Eq. (C.10) and rearranging the terms to suppress μ gives

$$\ln \frac{\theta_i}{\theta_o} = 0.092\ \frac{k_1^{0.2}}{c_{p1}^{0.2}\ Pr_1^{0.4}}\ \frac{D_1}{FD_2^2}\ D_e^{-0.2}\ G_1^{-0.2}\ L \ . \tag{C.15}$$

Taking

$$D_e = 4\ \frac{A_1}{\pi D_1} \ , \tag{C.16}$$

from Eqs. (C.16) and (C.11)

$$D_e = \frac{FD_2^2}{D_1} \ . \tag{C.17}$$

Substituting Eq. (C.17) into Eq. (C.15) gives

$$\ln \frac{\theta_i}{\theta_o} = 0.092 \left(\frac{k_1^{0.2}}{c_{p1}^{0.2}\ Pr_1^{0.4}}\right) \left(\frac{FD_2^2}{D_1}\right)^{-1.2} G_1^{-0.2}\ L\ . \qquad (C.18)$$

Solving for L

$$L = \frac{1}{0.092} \left(\frac{c_{p1}^{0.2}\ Pr_1^{0.4}}{k_1^{0.2}}\right) \left(\frac{FD_2^2}{D_1}\right)^{1.2} G_1^{0.2}\ \ln \frac{\theta_i}{\theta_o}\ . \qquad (C.19)$$

Appendix D

EVALUATION OF THE HEAT TRANSFER AREA FOR THE HEAT EXCHANGERS

Regenerator

The total mass flow rate (lb/hr) of the gas through the regenerator tubes is

$$M' = \frac{\pi}{4} D_2^2 G_2 N \ . \tag{D.1}$$

The total heat transfer area (ft^2) outside the tubes is

$$S_1 = \pi D_1 L N \ . \tag{D.2}$$

Eliminating N between Eqs. (D.1) and (D.2),

$$S_1 = \frac{4D_1}{D_2^2} \left(M' \frac{L}{G_2} \right) , \tag{D.3}$$

in ft^2. Taking $D_1 = 0.5/12$ ft and $D_2 = 0.4/12$ ft, Eq. (D.3) becomes

$$S_1 = \left(150 \frac{L}{G_2} \right) M' \equiv BM' \ , \tag{D.4}$$

where

$$B = 150 \frac{L}{G_2} \ .$$

Cooler

The total mass flow rate (lb/hr) of the gas through the cooler shell is

$$M' = A_1 G_1 N \ . \tag{D.5}$$

The total heat transfer area (ft^2) outside the tubes of the cooler is

$$S_1 = \pi D_1 L N \ . \tag{D.6}$$

Eliminating N between Eqs. (D.5) and (D.6),

$$S_1 = \frac{\pi D_1 L}{A_1 G_1} M' \ . \tag{D.7}$$

By definition of Eq. (C.11),

$$A_1 = \frac{\pi}{4} D_2^2 F \ . \tag{D.8}$$

From Eqs. (D.7) and (D.8),

$$S_1 = \left(\frac{4D_1}{D_2^2}\right) \frac{LM'}{FG_1} \ . \tag{D.9}$$

Taking $D_1 = 0.5/12$ and $D_2 = 0.4/12$,

$$S_1 = \left(150 \frac{L}{FG_1}\right) M' \equiv BM' \ , \tag{D.10}$$

where

$$B = 150 \frac{L}{FG_1} \ .$$

The B factors were evaluated from the data of Figs. 10 and 11 for the different values of the pumping power-to-heat removal ratio and the gas temperature rise (or drop). The total heat transfer area outside the tubes of the heat exchanger can be obtained by multiplying the total mass flow rate of the gas through the heat exchanger by the appropriate value of the B factor. A plot of B factors against the pumping power-to-heat removal ratio is shown in Fig. 12.

i

ORNL-3209
UC-80 — Reactor Technology
TID-4500 (41st ed.)

Internal Distribution

1. S. E. Beall
2. N. H. Briggs
3. C. E. Center (K-25)
4. C. W. Collins
5. F. L. Culler
6. W. R. Gall
7–18. A. P. Fraas
19. R. S. Holcomb
20. D. H. Jansen
21. C. E. Larson (K-25)
22. M. I. Lundin
23. H. G. MacPherson
24. J. F. Murdock
25. F. H. Neill
26. A. M. Perry
27. M. W. Rosenthal
28. G. Samuels
29. H. W. Savage
30. A. W. Savolainen
31. M. J. Skinner
32. J. R. Tallackson
33. W. C. Thurber
34–71. D. B. Trauger
72. D. R. Vondy
73. A. M. Weinberg
74–93. G. D. Whitman
94. J. Zasler
95–96. Central Research Library
97–98. Y-12 Document Reference Section
99–121. Laboratory Records Department
122. Laboratory Records, RC

External Distribution

123. W. R. Cooper, Tennessee Valley Authority, EGCR
124. W. E. Crowe, Los Alamos Scientific Laboratory
125. S. W. Doroff, Office of Naval Reserve, Washington, D.C.
126. N. R. Droulard, Technical Director, The Franklin Institute
127. Harold Falkenberry, Tennessee Valley Authority, Chattanooga
128. D. C. Kaulitz, Battelle-Northwest, Hanford
129. M. N. Ozisik, North Carolina State College, Raleigh, N.C.
130. J. H. Wright, Westinghouse Atomic Power Division, Pittsburgh, Pa.
131. J. F. Young, General Electric Atomic Power Division, San Jose, Calif.
132–133. General Atomic Library (Att.: R. B. Duffield, D. V. Ragone)
134–135. Reactor Division, AEC, ORO
136. Division of Research and Development, AEC, ORO
137–711. Given distribution as shown in TID-4500 (41st ed.) under Reactor Technology category (75 copies — CFSTI)